

17  
 ARCHIEF

*gth ONR*

<del>Bibliotheek van de Onderafdeling der Scheepsbouwkunde Technische Hogeschool, Delft</del>	
DOCUMENTATIE	: <i>K49-72/17</i>
DATUM:	9 OKT. 1973

*page 26*

Lab. v. Scheepsbouwkunde  
Technische Hogeschool  
Delft

*Scaling  
Offshore structure  
Forces  
Study*

DOCUMENTATIE  
02472

SOME ASPECTS OF VERY LARGE OFFSHORE STRUCTURES

by G. van Oortmerssen

Abstract

Due to the fast development of the offshore industry, there is a rapidly increasing demand for very large unconventional offshore structures, both floating and fixed to the bottom, to be applied for storage and production purposes. The general hydrodynamic aspects of these big objects will be summarized in this paper.

In the case of floating structures, the drift force is relatively important and consequently resonance phenomena can occur in the anchor lines. Therefore, in rather shallow water a structure fixed to the bottom will be preferred in many cases.

From calculations and model experiments it appeared, that the wave loading on a large object and the wave pattern around it can be calculated with great accuracy with a diffraction theory.

As an example a cylindrical storage tank - 96 m in diameter, fixed to the bottom in 50 m deep water and extending above the water surface - will be discussed.

Dutch Ship Model Basin

This example is hardly hypothetical, since structures with comparable dimensions are in the design stage or under construction at present.

The wave pressure on the tank and the wave diffraction as calculated with the potential theory are compared with measurements.

The agreement is very good.

From the wave pattern around the tank it was found, that it can be advantageous to moor a tanker immediately to the tank. Model tests were conducted with a tanker moored behind the tank in irregular seas, while the tanker motions and the force in the bowhawser were measured.

The results of these tests will be compared with the results of tests conducted with existing mooring systems.

## Introduction

The increasing importance of remote offshore oil fields has created a need for very large unconventional structures for production and storage of oil or liquid natural gas.

Some very large structures are now in use, as for instance the floating oil storage 'Pazargad' and the submerged tank in Dubai, while others are under construction, as for example the large concrete tank for the Ekofisk field in the North Sea. Besides structures for exploitation and storage of minerals, the use of very large offshore structures is considered for a variety of future purposes.

Plans exist to build polluting or dangerous plants on artificial islands, far from the living areas, to prevent a deterioration of the environmental conditions in densely populated industrial countries.

Fear for calamities and a need of plenty of cooling water was the reason to study the possibility to build offshore nuclear power plants, and there is even talk of constructing a floating intercontinental airport.

With regard to the design and construction of a large unconventional offshore structure, a lot of problems arise.

The structure has to be strong enough to survive the severest weather conditions.

In the case of floating structures, it is a problem to design a proper anchor system.

When the structure is fixed, the entire construction has to be stable.

In most cases, such artificial islands require trans-shipment of goods from ships to island or vice versa.

Consequently, attention has to be paid to the mooring of ships to the island.

If a construction on the sea bottom is considered, its behaviour during immersion has to be studied carefully.

In order to be able to cope with future developments, a research program has been performed at the Netherlands Ship Model Basin. A computer program has been developed for the calculation of wave loads on objects of arbitrary shape, using a three-dimensional source technique, while the effects of the free surface and of finite water depth were taken into account.

With this program it is also possible to calculate the wave pattern around the structure.

Subsequently model experiments were carried out to check the theoretical results.

Also the mooring of a tanker to a large circular storage tank was investigated by means of model tests.

In this paper the following topics will be discussed successively :

- the calculation of wave loads and wave diffraction, with a comparison of theoretical and experimental results ;
- anchoring of floating structures ;
- mooring of a ship to an artificial island.

The object is not to give practical solutions, but to scan the problems and possibilities which occur in the field of hydrodynamics.

## Wave - structure interaction

We shall consider the following aspects of the interaction between waves and a structure :

- the pressure distribution on the surface of the body, which has to be known for the structural design ;
- the total wave excited forces and moments, which are important for the design of an anchor system in the case of a floating structure, or, if the body is fixed, for the stability of the structure : the amplitude of the vertical force, for instance, must be smaller than the apparent weight of the structure in the case of a submerged structure fixed to the bottom ;
- the wave diffraction : if ships are to moor to the structure, it is important to know in which way the incident waves are deformed by the presence of the structure.

The interaction between waves and a structure is governed by inertial, gravitational and viscous effects.

The relative importance of each of these effects depends on the ratios of the wave height and the wave length to the body dimensions.

In Figure 1 the regions of influence of the different effects are indicated for the case of a vertical circular cylinder (See ref. [1]).

From this Figure it appears, that gravitational effects must be taken into account if  $ka$  is larger than 0.6 , or in general, if the wave length is smaller than approximately five times the body dimensions.

This means that, for the structures with which we are dealing here, both the inertial and gravitational effects must be considered.

These phenomena can be described adequately by means of the potential theory ; this theory, however, presupposes an inviscid fluid.

Fortunately, it can be stated that for large structures the potential forces are predominant to such a degree, that the viscous effects can be neglected.

Potential theory approach

Consider a fluid, bounded by a partially or totally submerged rigid body, a fixed bottom and a free surface.

The undisturbed free surface will be taken as XOY-plane of the co-ordinate system, with the z-axis pointing vertically upwards. The fluid is assumed to be inviscid, incompressible and irrotational.

All motions will be infinitely small.

At infinity the fluid motion behaves as a single harmonic wave, travelling in the positive direction of the x-axis.

If the undisturbed wave has a frequency  $\omega$ , the velocity potential may be written as :

$$\phi = \text{Re} [\varphi e^{-i\omega t}] \dots\dots\dots(1)$$

The function  $\varphi$  has to satisfy the Laplace equation :

$$\nabla^2 \varphi = 0 \dots\dots\dots(2)$$

and the boundary conditions :

- at the bottom  $\frac{\partial \varphi}{\partial z} = 0$  for  $z = -d$  .....(3)

- in the free surface  $\frac{\partial \varphi}{\partial z} = v\varphi$  for  $z = 0$  .....(4)

- at the body contour  $\frac{\partial \varphi}{\partial n} = 0$  for  $\underline{x} = \underline{s}$  .....(5)

in which :

d = water depth

v =  $\omega^2 / g$

g = the acceleration of gravity

s = vector which describes the body contour

n = vector normal to the contour

The function  $\varphi$  can be split into two components :

$$\varphi = \varphi_i + \varphi_s \dots\dots\dots(6)$$

in which :

- $\varphi_i$  = the wave function of the undisturbed incident waves
- $\varphi_s$  = the wave function of the scattering waves

Both components have to satisfy the Laplace equation. The function for the incident wave, including the boundary conditions in the free surface and at the bottom, is given by :

$$\varphi_i = \frac{\zeta_a g}{\omega} \frac{\cosh k (d + z)}{\cosh kd} e^{ikx} \dots\dots\dots(7)$$

in which :

- $\zeta_a$  = incident wave amplitude
- $k$  = wave number =  $2\pi/\lambda$
- $\lambda$  = wave length

The relation between wave frequency and wave length is given by the dispersion equation :

$$\omega^2 = kg \tanh kd \dots\dots\dots(8)$$

The wave function  $\varphi_s$ , corresponding to the motion of the scattered waves must, besides the boundary condition in the free surface and at the bottom, also satisfy the radiation condition. This condition requires that, at infinity,  $\varphi_s$  behaves as a radially outgoing progressive wave and imposes a uniqueness which would otherwise not be present.

In a system of local axes with cylindrical co-ordinates  $r, \theta$  and  $z$ , the radiation condition can be formulated as :

$$\lim_{r \rightarrow \infty} r^{1/2} \left( \frac{\partial \phi_s}{\partial r} - i v \phi_s \right) = 0 \dots\dots\dots(9)$$

in which :

$$r = (x^2 + y^2)^{1/2}$$

$$\theta = \arctan (y / x)$$

Analytical solutions

An analytical solution of the potential function can only be given for certain bodies of which the geometry can be described by means of a simple mathematical formula, such as the cylinder, the sphere and the ellipsoid.

Havelock [2] for instance, has given the solution for an infinitely long vertical cylinder of circular section.

This solution has been adapted for a cylinder fixed to the bottom in shallow water by Mac Camy and Fuchs [3] and Flokstra [4].

According to Flokstra, the analytical solution of the potential in cylindrical co-ordinates is - for this particular case - given by :

$$\phi(r, \theta, z, t) = \frac{\zeta_a g}{\omega \cosh kd} \cosh k(z + d) e^{-i\omega t} \sum_{n=0}^{\infty} \epsilon_n C_n (i)^{+n} \cos n\theta \dots\dots\dots(10)$$

in which :

$$C_n = i \frac{J_n(kr) Y_{n,r}(ka) - J_{n,r}(ka) Y_n(kr)}{J_{n,r}(ka) + i Y_{n,r}(ka)}$$

$$\epsilon_n = 1 \text{ for } n = 0$$

$$\epsilon_n = 2 \text{ for } n \neq 0$$



For the case that the cylinder does not extend to the bottom, Garret [5] has derived an analytical solution, using variational principles.

Numerical solutions

For a body of arbitrary shape, the velocity potential can be found from numerical methods.

At the Netherlands Ship Model Basin a computer program has been developed for the numerical calculation of the velocity potential, using a source distribution over a surface inside the body.

According to Lamb [6] the potential function can be found from :

$$\varphi_s(\underline{x}) = \iint_A q(\underline{a}) \gamma(\underline{x}, \underline{a}) dA \dots\dots\dots(11)$$

in which :

- $\gamma(\underline{x}, \underline{a})$  = the Green's function for a source, singular in  $\underline{a}$
- $\underline{a}$  = vector which describes the surface A, on which the sources are located
- $q(\underline{a})$  = the unknown source strength

The Green's function represents the contribution to the velocity potential in  $\underline{x}$  due to a unit wave source located in  $\underline{a}$ .

A Green's function which satisfies the boundary conditions in the free surface, at the bottom and the radiation condition, has been given by John [7] :

$$\begin{aligned} \gamma(\underline{x}, \underline{a}) = & 2\pi \frac{k^2 - v^2}{k^2 d - v^2 d + v} \cosh k(c+d) \cosh(z+d) \left[ Y_0(kr_j) - iJ_0(kr_j) \right] \\ & + \sum_{n=1}^{\infty} \frac{4(k_n^2 + v^2)}{dk_n^2 + dv^2 - v} \cdot \cos k_n(z+d) \cos k_n(c+d) K_0(k_n r_j). \end{aligned}$$

.....(12)

in which :

$$r_j = \sqrt{(x - a)^2 + (y - b)^2}$$

$$k_n \tan(k_n \cdot d) + v = 0$$

The source strength  $q(\underline{a})$  can be obtained after substitution of (11) in the boundary condition at the body surface :

$$\frac{\partial \phi}{\partial n} = \frac{\partial \phi_1}{\partial n} + \frac{\partial \phi_2}{\partial n} = 0 \text{ for } \underline{x} = \underline{s} \dots\dots\dots(13)$$

or :

$$\frac{\partial}{\partial n} \left\{ \iint_A q(\underline{a}) \cdot \gamma(\underline{x}, \underline{a}) dA \right\} = - \frac{\partial \phi_1(\underline{x})}{\partial n} \text{ for } \underline{x} = \underline{s} \dots\dots\dots(14)$$

For a restricted number of discrete sources, this integral equation changes into a set of linear equations in the unknown source strengths .

For an infinitely great number of sources, the numerical solution approaches the exact solution.

It will be clear that the accuracy obtained in the calculations depends on the number of sources applied and on the location of the sources.

Pressure, forces and wave diffraction

Once the velocity potential is known, the different aspects of the interaction between structure and waves can be calculated without much difficulty.

According to Bernoulli's theorem, the pressure is given by :

$$p = F(t) - \rho g z + \rho \frac{\partial \phi}{\partial t} + \frac{1}{2} \rho \left\{ \left( \frac{\partial \phi}{\partial x} \right)^2 + \left( \frac{\partial \phi}{\partial y} \right)^2 + \left( \frac{\partial \phi}{\partial z} \right)^2 \right\} \dots\dots\dots(15)$$

The dynamic wave load on the structure is given by the linearized pressure :

$$p = \rho \frac{\partial \phi}{\partial t} \dots\dots\dots(16)$$

The total wave excited forces (and moments) can be found by integration of the pressure over the surface of the body. The total force is composed of a periodic and a constant part. The oscillating part of the wave force is found from the linearized pressure :

$$\underline{F} = \iint_A p(\underline{x}) \cdot \underline{n} \cdot dA \dots\dots\dots(17)$$

Similarly we find for the moment :

$$\underline{M} = \iint_A p(\underline{x}) \cdot \{ \underline{x} \times \underline{n} \} dA \dots\dots\dots(18)$$

The constant part of the wave force or drift force can be found from :

$$\underline{F}_c = \frac{1}{2} \rho \iint_A \left\{ \left( \frac{\partial \phi}{\partial x} \right)^2 + \left( \frac{\partial \phi}{\partial y} \right)^2 + \left( \frac{\partial \phi}{\partial z} \right)^2 \right\} \cdot \underline{n} \cdot dA \dots\dots\dots(19)$$

Evaluation of this integral results in a constant term plus higher harmonic components, which can be neglected.

Although the constant force is a second order effect, Havelock [2] has shown that this force may be determined, using a first order approximation for the velocity potential.

In general, the constant force is small in comparison with the oscillating wave force; for large structures, however, it may become of interest.

The wave pattern due to the diffraction of waves by the object can also be found from Bernoulli's theorem.

In the free surface, the linearized pressure has to be zero, hence :

$$p = - \rho g z + \rho \frac{\partial \phi}{\partial t} = 0 \dots\dots\dots(20)$$

Consequently we find for the surface elevation :

$$\zeta = - \frac{1}{g} \left\{ \frac{\partial \phi}{\partial t} \right\}_{z=0} \dots\dots\dots(21)$$

### Comparison of theoretical and experimental results

Model tests were performed at the Netherlands Ship Model Basin in order to check the theoretical calculation of wave forces, pressure and wave diffraction.

In Figures 2 and 3 the oscillating horizontal and vertical wave forces on a circular cylinder, as calculated with the computer program of the Netherlands Ship Model Basin, using the three-dimensional source technique, are compared with experimental results.

The experimental values, which are given in these Figures, were obtained from cross-fairing of the results of a great number of measurements, which were performed with systematically varied cylinders.

Also given in these Figures are the values according to the analytical solution of Garret.

The results of the numerical calculations, which were obtained using only 42 sources to represent the cylinder, closely approximate the analytical results of Garret, while there is also a good agreement between the theoretical and experimental results.

From the measurements of the total horizontal wave force on the cylinders, the mean value which represents the constant resistance or drift force, was also determined.

In Figure 4 the results are given for a particular case, together with the calculated values.

In order to check a more extreme case, calculations and measurements were performed for a pyramid-like structure, of which the shape is given in Figure 5.

Due to the sharp edges, it is difficult to represent this object by means of a source distribution.

The number of sources, applied in the computer calculations, amounts to 92.

The results of the calculations and the measurements of the horizontal wave force on the structure are given in Figure 6. Even in this case the agreement is reasonable.

Some aspects of the interaction between structure and waves were studied in greater detail for a circular model, which - at a scale ratio of 1 : 100 - can be regarded as the representation of a cylindrical island, for instance a storage tank, 96 m in diameter, fixed to the bottom in 50 m deep water and extending to above the water surface.

The pressure distribution on this model was determined in regular waves with varying periods.

To this end the model was provided with four very sensitive pressure gauges. These gauges were placed on a vertical line at regular distances, to obtain the distribution of the pressure over the water depth.

The measurement of the variation of the pressure along the circumference of the cylinder was established by rotating the model.

In Figures 7 and 8 the results are given for  $ka = 2$  and  $ka = 3$ , which for a scale ratio of 1 : 100, correspond to wave periods of 8 and 10 seconds.

In general, the measured pressures closely approximate the calculated values.

The diffraction of the waves by the cylinder was calculated with the potential theory and also measured in the basin in a large number of points around the model.

Figure 9 shows the calculated wave pattern for  $ka = 1.4$ .

The lines in this Figure connect the points with equal values of the ratio of resulting wave height to incident wave height. In Figures 10 and 11 the results are given of the calculated and measured wave height behind and in front of the cylinder for  $ka = 4$ .

Again, the experiments confirm the theoretical calculations.

### Wave loads in high, irregular and breaking waves

Up till now only sinusoidal waves of low amplitude were taken into consideration.

However, for the design of offshore structures, the maximum wave condition is important ; such a condition usually is an irregular sea-state, consisting of high waves, among which sometimes even breaking waves will occur.

High regular waves are not sinusoidal any longer, the distance of the crest to the still water level becomes greater than the distance of the trough to the still water level.

However, a steep regular wave can always be split up into a number of harmonic components.

From various experiments the experience was gained, that the forces and pressures in high waves can be found by summation of the forces and pressures, as calculated for the different components according to the potential theory for sinusoidal waves of low amplitude.

In non-periodic waves, as far as the linear phenomena are concerned, force and pressure spectra can be calculated, departing from the wave energy spectrum and the force and pressure response functions.

In such a statistic approach, no data can be obtained with regard to drift forces.

Since the magnitude of the drift force is proportional to the square of the wave height and also dependent on the wave frequency, this force is no longer constant in irregular seas and is thus known as the slowly oscillating drift force which has a period of oscillation in the order of magnitude of ten times the mean wave period.

For an estimation of the drift force a deterministic approach can be applied (see Hsu and Blenkarn [5] and also Remery and Hermans [9]). In this approach the point of departure is not the energy spectrum of the waves, but a record of the wave height to a base of time, which can be obtained either by field measurements, or by calculations, in which case one of the possible realizations of a spectrum is generated by a computer.

The wave record can be regarded as a sequence of separate wave crests and troughs, each with its own period and amplitude. For every part of the wave record the drift force can be calculated, resulting in a record of the drift force to a base of time.

The drawback of this method is, that no indication is obtained about the chance of exceeding a certain force. The maximum force, encountered in a certain wave train, will differ from the maximum force in an other wave train with the same energy distribution.

No theoretical approach is available for the determination of peak loads, which can occur in breaking waves.

In [10] Wiegel gives a review of experimental work performed on this topic.

Most of the investigations were related to the phenomena which occur when a wave breaks against a vertical barrier ; a smaller part was concerned with cylinders in breaking waves.

From the laboratory tests with vertical barriers it appeared, that when a breaking wave hits the wall, the chance that a peak load occurs is about two per cent.

Wave induced impact forces only occur, when the wave breaks just at the wall, while trapping a thin lense of air.

Apparently, the energy of the impact is stored in the compression of the air cushion.

Therefore, it is very unlikely that peak forces will occur if the surface of the object is curved.

In the case of large structures with flat or practically flat walls, the possibility that peak loads occur due to breaking waves, must be taken into account.

The magnitude of the peak loads can only be found by means of experiments.

The anchoring of floating structures

The anchoring of very large floating structures involves tremendous problems, since the anchor system must be able to survive the severest weather conditions.

In high waves the drift force becomes very important and causes a high mean load in the anchor lines.

Due to the non-linear characteristic of the anchor system - which is schematically shown in Figure 12 - the spring constant increases considerably by this mean load and consequently the oscillating motion of the structure induces high oscillating forces in the anchor lines.

Let us consider, as an example, a circular storage tank - 120 m in diameter, with a draft of 25 m and a displacement weight of approximately 290,000 ton - which is anchored in a water depth of 40 m.

It was calculated that, in a design wave with a height of 20 m and a period of 19 seconds, this structure is subjected to a drift force of 4,730 ton and an oscillating force with an amplitude of 58,900 ton.

If it is assumed that the motion of the structure is a pure surge motion and that the damping can be neglected, the motion can be described by :

$$m_v \ddot{x} + cx = F_{xa} \cdot e^{-i\omega t} \dots\dots\dots(22)$$

in which :

- $m_v$  = the virtual mass
- $c$  = the spring constant in x-direction of the anchor system
- $F_{xa}$  = the amplitude of the oscillating wave excited force in x-direction

Since the relation between the force and excursion of the anchor system is non-linear, this equation has no simple analytical solution.



Due to the drift force, the motion of the structure will be an oscillating motion around a point which is situated in the steep part of the load-excursion curve, as indicated in Figure 12.

The relevant part of the curve may be regarded as linear with an inclination c.

Consequently, the resulting surge motion is given by the linear approximation of equation (22) :

$$x = x_a \cdot e^{-i\omega t} \dots\dots\dots(23)$$

in which :

$x_a$  = the amplitude of the motion

After substitution of (23) in (22), we find that the amplitude of the surge motion will be :

$$x_a = \frac{F_{xa}}{|c - m_v \omega^2|} \dots\dots\dots(24)$$

The resulting maximum reaction force in the anchor system becomes :

$$F_{Rx \text{ max.}} = 4,730 + x_a \cdot c \dots\dots\dots(25)$$

In Figure 13 the maximum reaction force in x-direction is given to a base of the spring constant.

From this Figure it becomes obvious that it will be very hard in this case to design a proper anchor system.

Resonance will occur if :

$$c = m_v \omega^2 \dots\dots\dots(26)$$

and, since most of the wave energy is related to wave frequencies between  $\omega = 0.2$  and  $\omega = 1.0$ , values of c between 2,400 and 60,000 ton/m should be avoided.

A value of  $c$  higher than 60,000 ton/m means an almost rigid connection to the sea bottom, which must be able to absorb a horizontal force of over 60,000 ton ; this does not seem to be a practical solution.

On the other hand, if  $c$  is chosen to amount to less than 2,400 ton/m, the risk exists that in irregular seas the slowly varying drift force induces resonance phenomena.

In reality the problem is much more complicated than was assumed in this simple calculation : besides the surge motion, also heave and pitch may be of importance, and due to the high waves, the drift force and the characteristics of the anchor system , the motions will be non-linear.

Therefore, model tests are indispensable to investigate the anchoring of large structures.

The above example has shown, however, that enormous problems are involved with the anchoring of very large structures with a small length to breadth ratio.

Therefore, in rather shallow water, a structure fixed to the bottom, will be preferred in many cases.

If a floating structure is required - for instance because there exists a risk of earthquakes - or if the structure has to be more or less mobile, it is desirable to choose a shape with a minimum drift force, as for example a ship-shaped structure moored to a single point mooring system or a semi-submersible structure.

### Mooring of a ship to a large structure

For the oil storage tanks which are now in use or under construction, a concept was selected by which the loading tanker is not moored immediately to the storage tank, but to a separate single buoy mooring system.

If we consider the wave pattern around the circular tank, as given in Figure 9, regions where the waves are higher, as well as regions where the waves are lower than the incident waves, can be observed.

For other wave lengths, the wave pattern changes, but there is always an area behind the structure where the waves are lower than the incident waves. It can therefore be expected, that the diffraction of waves by a large fixed structure will be advantageous when a ship is moored immediately behind it.

In order to investigate the behaviour of a tanker, moored to a storage tank by means of a bowhawser, a model test program was performed at the Netherlands Ship Model Basin with the cylindrical model - discussed already in a previous section - and a model of a tanker with a displacement of approximately 100,000 ton. The main particulars of the tanker are given in Table I, while Figure 14 shows a small scale body plan.

The weight distribution and stability characteristics of the tanker were reproduced to scale.

The tanker was moored to the storage tank by means of a single bowhawser, representing a nylon mooring line with a breaking strength of 150 ton and a length of 50 m.

The load-elongation characteristic of this bowhawser is given in Figure 15.

The following tests were performed :

- a. Measurement of the wave height in regular and irregular seas behind the structure, at the position of the midship section of the tanker ;
- b. Measurement of the mooring line force and of the surge and heave motions of the bow of the tanker with the tanker moored to the cylindrical tank in irregular seas ;
- c. Measurement of the mooring line force and of the motions of the bow of the tanker with the tanker moored to a fixed pile of small diameter, in the same sea-states as tests b.

These tests were performed in order to determine the influence of the wave diffraction on the behaviour of the moored ship.

The different test arrangements are shown in Figure 16.

For the measurement of the wave height a wave transducer of the resistance type was used.

The force in the bowhawser was measured by means of a strain gauge transducer and the surge and heave motions of the tanker by means of a pantograph.

The measurements in irregular seas lasted 210 seconds or 35 minutes for the full scale, which is regarded to be long enough to obtain reliable statistic data.

Besides the measurements, the wave diffraction at the position of the midship section of the tanker was also calculated with the potential theory.

In Figure 17 the calculated ratio of wave amplitude behind the cylinder to incident wave amplitude  $\zeta_a^*/\zeta_a$  is given to a base of the wave frequency  $\omega$ , together with some experimental values. With the aid of this curve of  $\zeta_a^*/\zeta_a$ , the energy spectrum behind the cylinder can be calculated for any incident wave spectrum.

The spectral density  $S_{\zeta}$  of the incident waves is defined by :

$$S_{\zeta}(\omega_n) d\omega = \frac{1}{2} \zeta_{an}^2 \dots\dots\dots(27)$$

in which :

$\zeta_{an}$  = the amplitude of the nth component of  $\zeta(t)$  with circular frequency  $\omega_n$ .

Consequently, the spectral density of the waves at the position of the midship section of the tanker can be found from :

$$S_{\zeta}^* (\omega_n) d\omega = \frac{1}{2} \zeta_{an}^2 \left[ \frac{\zeta_{an}^* (\omega_n)}{\zeta_{an}} \right]^2 \dots\dots\dots(28)$$

or

$$S_{\zeta}^* (\omega_n) = S_{\zeta} (\omega_n) \left[ \frac{\zeta_{an}^* (\omega_n)}{\zeta_{an}} \right]^2 \dots\dots\dots(29)$$

In Figures 18, 19 and 20 the spectral densities of the sea-states applied during the tests, are given together with the predicted and measured spectral densities behind the cylinder.

There is a good agreement.

The tests with the moored tanker were performed in the spectra 2 and 3, with significant wave heights of 3.36 m and 5.05 m. The most important test results are stated in Table II.

The most remarkable outcome of the experiments is the considerable reduction in the mooring line force, due to the presence of the cylindrical structure.

The reduction in the force is relatively much higher than the reduction in the wave height.

This can possibly be explained by the fact, that the drift force plays an important role in the behaviour of a moored ship, this drift force being proportional to the square of the wave height.

If, for instance, we have a wave with frequency  $\omega = 0.8$ , it follows from Figure 17, that the wave height is decreased by 20 per cent. at the position of the moored tanker, and consequently the drift force is decreased by 36 per cent. compared with the drift force in the undisturbed waves.

In Figure 21 the results of the present tests are compared with results obtained from the statistics of tests performed at the Netherlands Ship Model Basin with different single point mooring systems.

For this comparison the following dimensionless coefficients were applied :

- for the mooring line force 
$$\frac{F_s^{1/3}}{\rho g \nabla^{2/3} \zeta_w^{1/3}}$$

and

- for the wave frequency 
$$\omega \sqrt{L_{pp}/g}$$

in which :

$\nabla$  = the displacement volume

$L_{pp}$  = the length between perpendiculars

Due to the non-linear characteristic of the bowhawser, the significant force is not proportional to  $\nabla^{2/3}$  and  $\zeta_w^{1/3}$ , and therefore only results of tests with tankers of comparable size in comparable sea-states were selected.

From Figure 21 it appears, that the results obtained with the tanker moored to a fixed point represent approximately the lower limit of the results of conventional single point mooring systems. The forces occurring in the mooring line when the tanker is moored behind the cylindrical storage tank, are much lower than those for all other considered systems.

These model tests have shown that it is advantageous to moor a ship immediately behind a large fixed structure, though it should be admitted that a rather simple case was considered, since the additional effect of current or wind from a direction different from the wave direction was not investigated.

## Conclusions

1. The wave loads on large structures due to non-breaking waves can be predicted fairly accurately by means of a three-dimensional source theory.
2. For the study of the anchoring of large structures or the mooring of ships to large structures, an entirely theoretical approach is not feasible and consequently model experiments are required.
3. Very large floating structures anchored in exposed areas should preferably be either slender or semi-submersible ; large structures with a small length to breadth ratio will require extremely heavy anchoring equipment.
4. Mooring a ship on the lee-side of a fixed structure can be of advantage.  
If the ship is moored to the structure by a single bowhawser, the force in the latter will be smaller than the force which would occur in a conventional single point mooring system.



References

- [1] Cortmerssen, G. van :  
'The interaction between a vertical cylinder and regular waves',  
Symposium on 'Offshore Hydrodynamics', Wageningen (August 1971).
- [2] Havelock, T.H. :  
'The pressure of water waves upon a fixed obstacle',  
Proc. of the Royal Society of London, Series A - No. 963  
Vol. 175 (1940).
- [3] Mac Camy, R.C. and Fuchs, R.A. :  
'Wave forces on piles : a diffraction theory',  
Technical Memorandum No. 69, Beach Erosion Board (1954).
- [4] Flokstra, C. :  
'Wave forces on a vertical cylinder in finite water depth',  
N.S.M.B. Report No. 69-107-WO, Wageningen (September 1969).
- [5] Garret, C.J.R. :  
'Wave forces on a circular dock',  
Journal of Fluid Mechanics - Vol. 46 (1971).
- [6] Lamb, H. :  
'Hydrodynamics',  
Sixth Edition (1932).
- [7] John, F. :  
'On the motion of floating bodies',  
Comm. on Pure and Applied Mathematics, 3 (1950).

- [3] Hsu, F.H. and Blenkarn, K.A. :  
'Analysis of peak mooring forces caused by slow vessel  
drift oscillation in random seas',  
Offshore Technology Conference, Houston (1970).
- [9] Remery, G.F.M. and Hermans, A.J. :  
'The slow drift oscillations of a moored object in  
random seas',  
Offshore Technology Conference, Houston (1971).
- [10] Wiegel, R.L. :  
'Oceanographical Engineering',  
Prentice-Hall, Englewood Cliffs (1965).

Nomenclature :

$a$	= cylinder radius
$c$	= spring constant of the anchor system
$d$	= water depth
$\underline{F}$	= oscillating wave excited force
$F_{cx}$	= drift force
$F_R$	= reaction force of the anchor system
$F_{xa}$	= amplitude of the horizontal wave excited force
$F_{za}$	= amplitude of the vertical wave excited force
$g$	= acceleration due to gravity
$h$	= draught
$J_n$	= Bessel function of the first kind of order $n$
$J_{n,r}$	= derivative of $J_n$ with respect to $r$
$k$	= wave number
$K_n$	= modified Bessel function of the second kind of order $n$
$L_{pp}$	= length between perpendiculars
$\underline{M}$	= oscillating wave excited moment
$p$	= pressure
$q$	= source strength
$S_\zeta$	= spectral density of the waves
$Y_n$	= Weber's Bessel function of the second kind of order $n$
$Y_{n,r}$	= derivative of $Y_n$ with respect to $r$
$\lambda$	= wave length

- $\omega$  = circular frequency
- $\bar{\omega}$  = mean circular frequency in irregular waves
- $\rho$  = fluid density
- $\gamma$  = Green's function
- $\phi$  = velocity potential
- $\psi$  = wave function
- $\psi_i$  = wave function of the incident waves
- $\psi_s$  = wave function of the scattering waves
- $v$  =  $\omega^2 / g$
- $\zeta$  = wave elevation
- $\zeta_a$  = incident wave amplitude
- $\zeta_a^*$  = local wave amplitude
- $\zeta_w$  = wave height (crest to trough)
- $\nabla$  = volume of displacement

Table I: Main particulars of the tanker

Designation	Symbol	Unit	
Length between perpendiculars	$L_{pp}$	m	249.38
Breadth	B	m	37.41
Draft (even keel)	T	m	13.85
Volume of displacement	$\nabla$	$m^3$	106,792
Displacement weight in sea water	$\Delta$	tons	109,462
Block coefficient	$C_B$	-	0.826
Midship section coefficient	$C_M$	-	0.985
Longitudinal radius of gyration	$k_{\theta\theta}$	m	58.61
Transverse radius of gyration	$k_{\phi\phi}$	m	8.98
Centre of buoyancy before midship section	f	m	3.78
Centre of gravity above keel	$\overline{GK}$	m	10.09
Metacentric height	$\overline{GM}$	m	5.55

Table II: Results of the mooring tests

Test arrangement B = Tanker moored to the cylindrical tank

Test arrangement C = Tanker moored to a fixed point

Test arrangement	Wave spectrum		Significant force in bowhawser	Surge			Heave
	$\bar{\omega}_{w1/3}$ in m	$\bar{T}$ in sec.		$\bar{x}_{a1/3} +$	$\bar{x}_{a1/3} -$	$\bar{x}$	
B	5.05	9.98	28.0	-2.37	-10.63	-6.39	3.40
B	3.36	7.96	7.0	-1.06	-3.14	-1.99	1.06
C	5.05	9.98	51.6	-7.23	-13.19	-10.04	3.85
C	3.36	7.96	8.3	-0.92	-3.21	-2.23	0.89

The bowhawser force is given in metric tons

The motions are given in metres

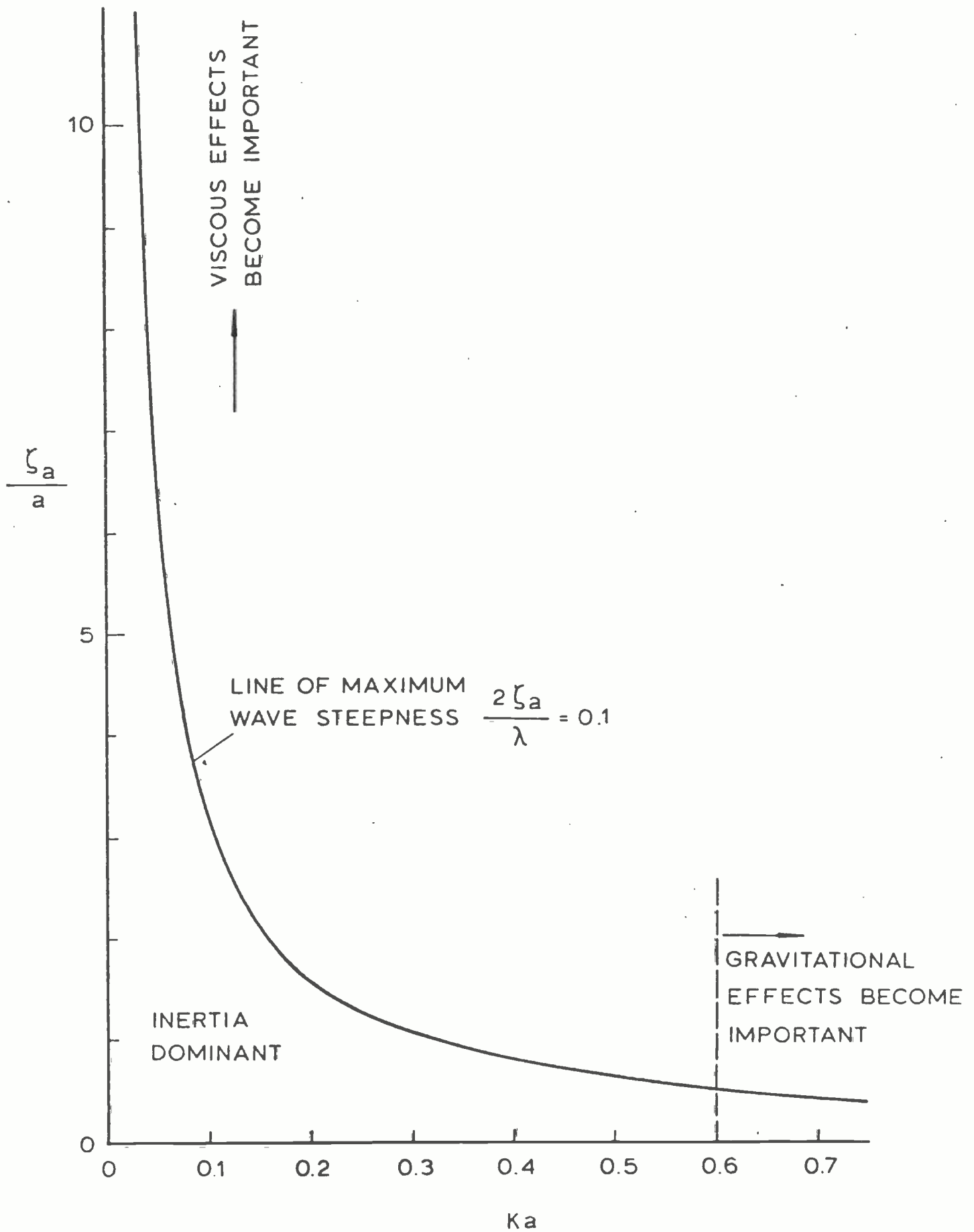


Fig. 1 Regions of influence of inertia, gravity and viscosity for a vertical circular cylinder with radius  $a$ .

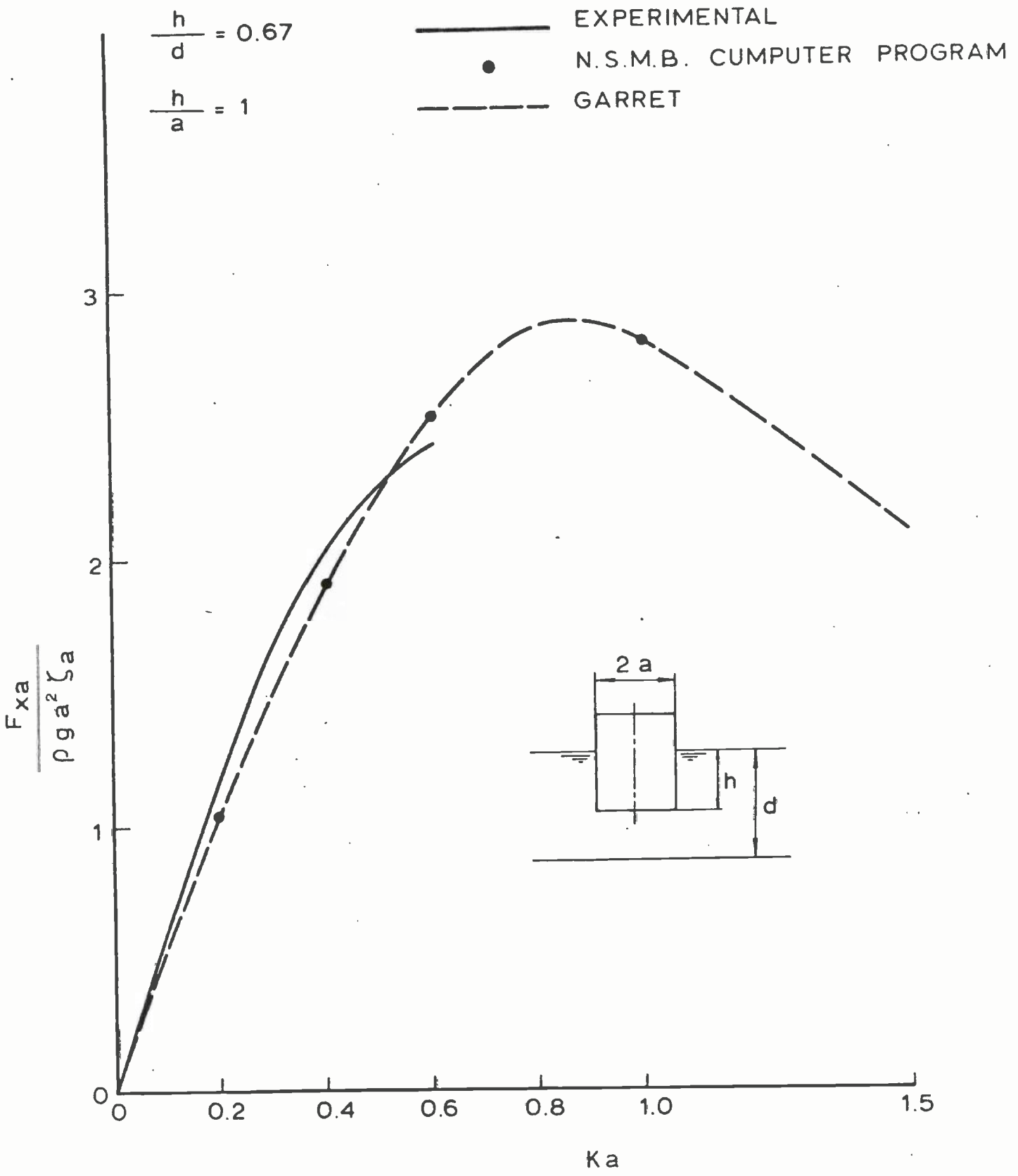


FIG. 2 Oscillating horizontal wave force on a circular cylinder.



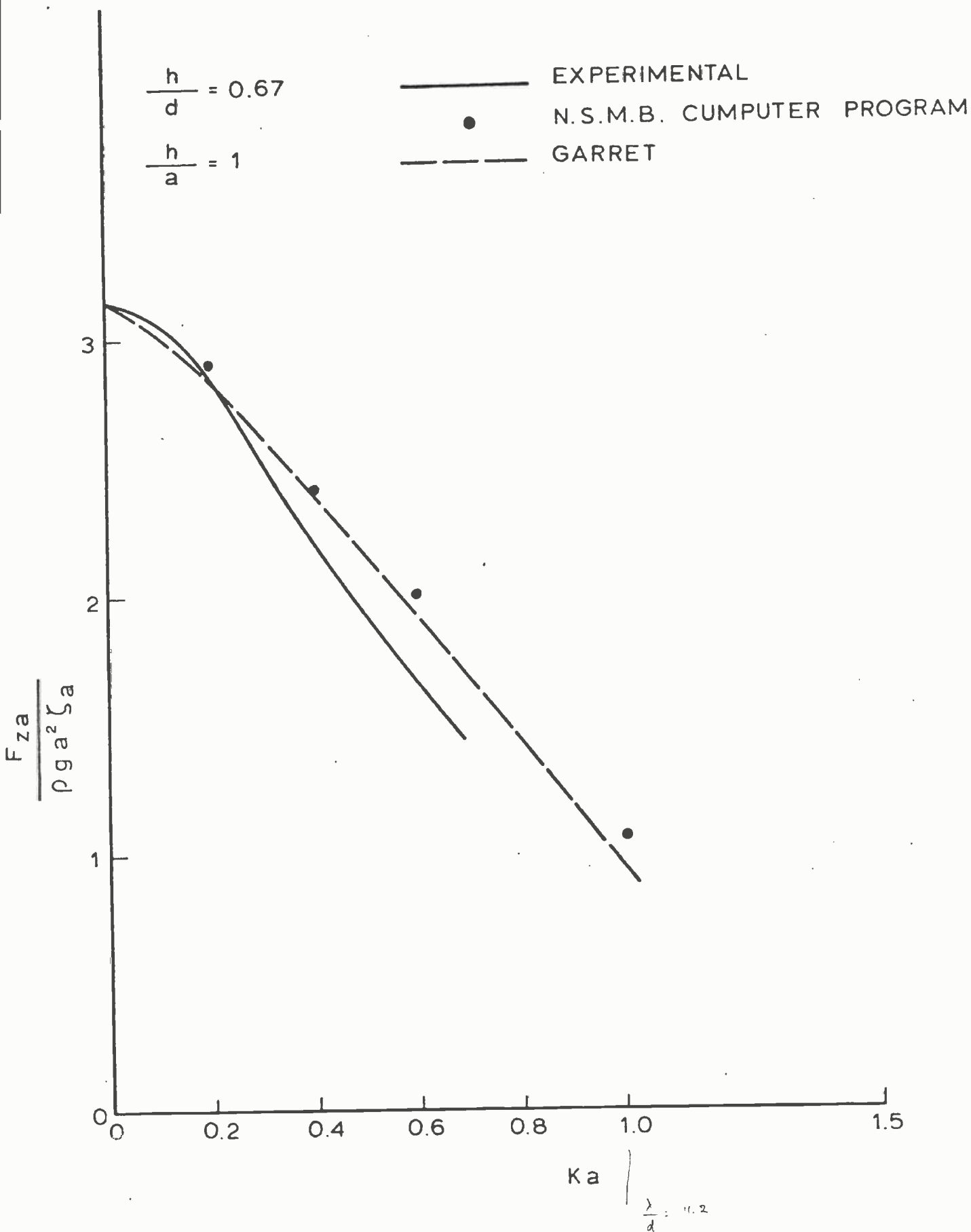


FIG. 3 Oscillating vertical wave force on a circular cylinder.

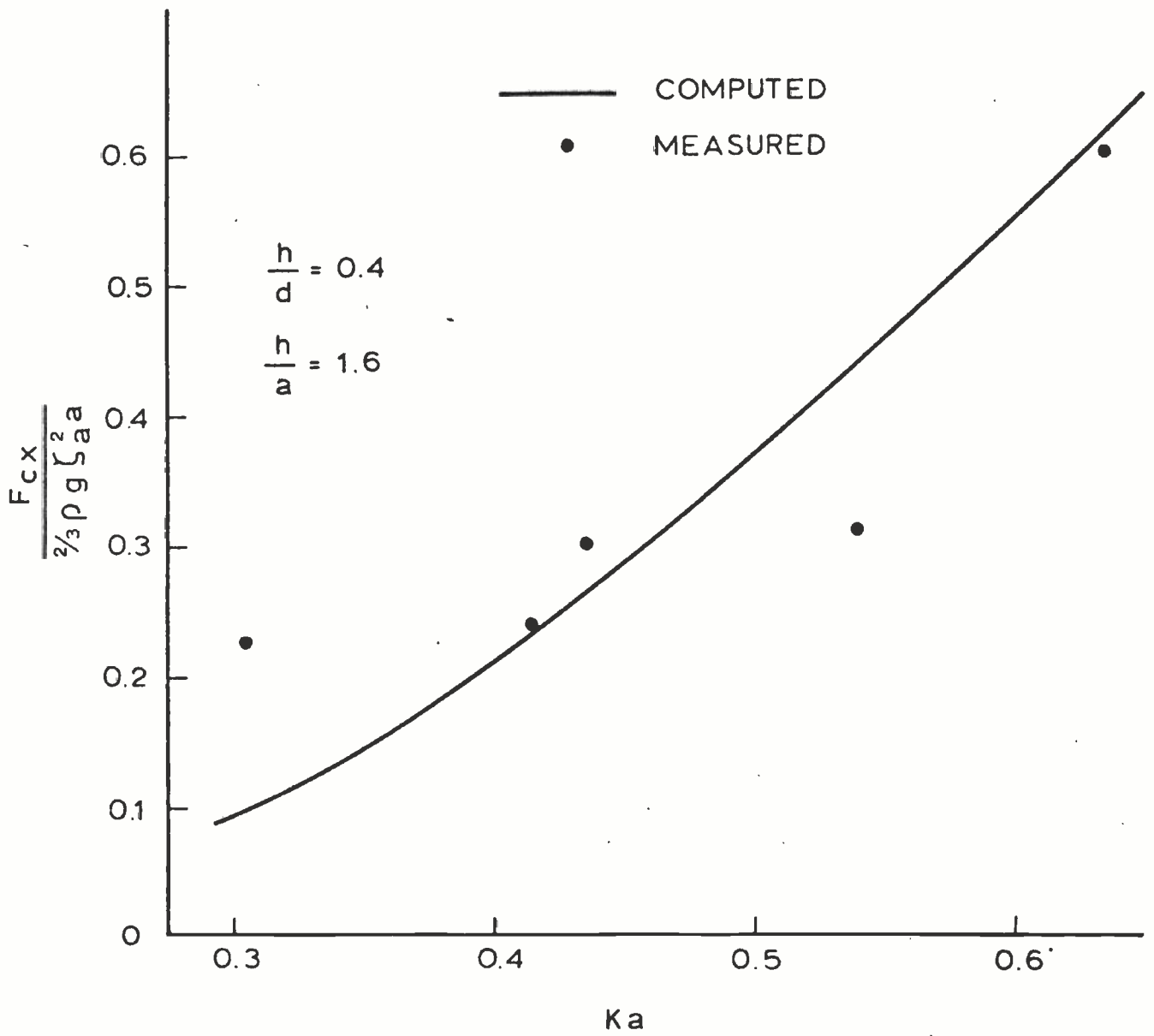


Fig. 4 Drift force on a circular cylinder.

DIMENSIONS in millimetres

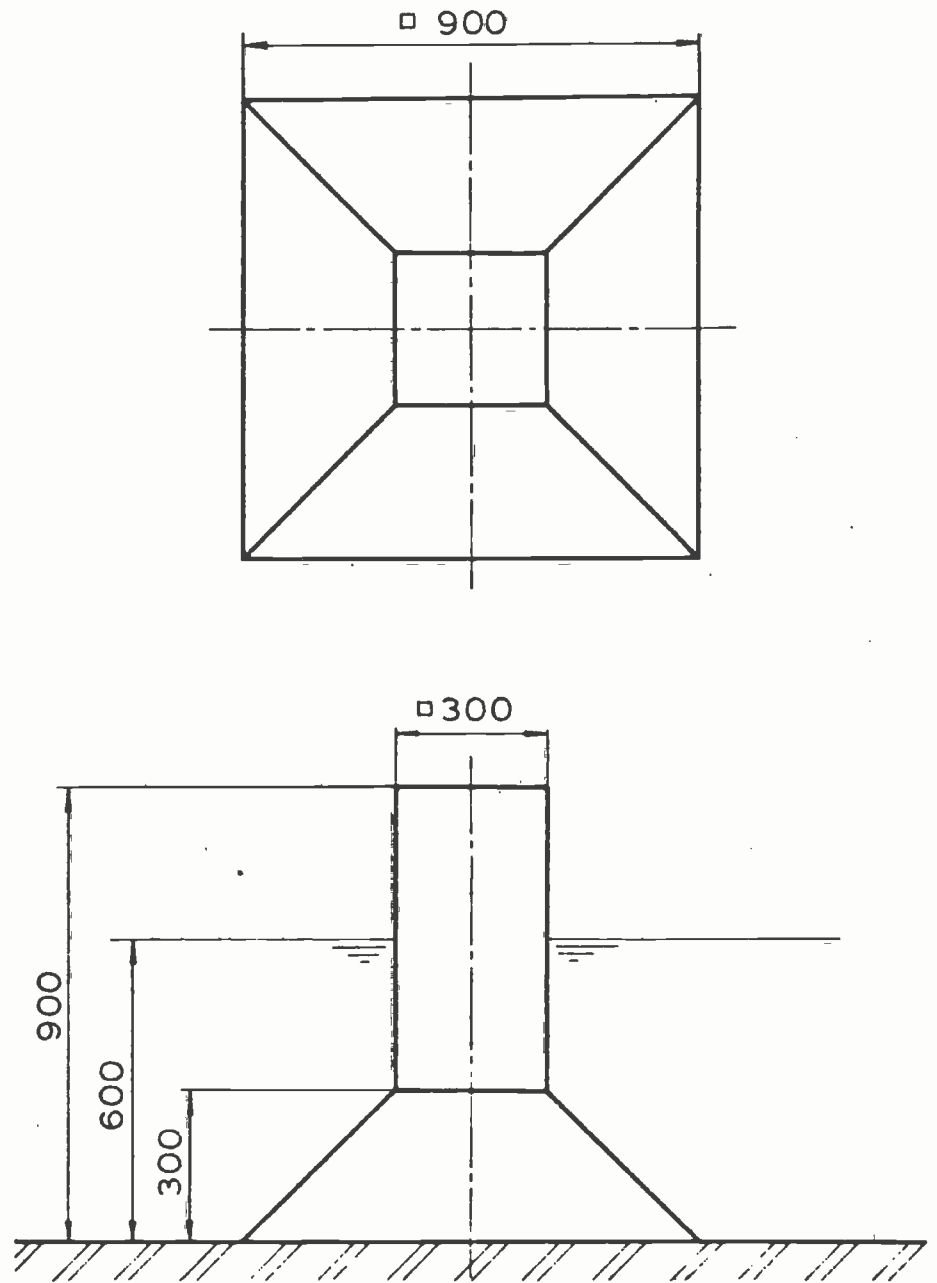


Fig. 5 Outline of the pyramid-shaped model.

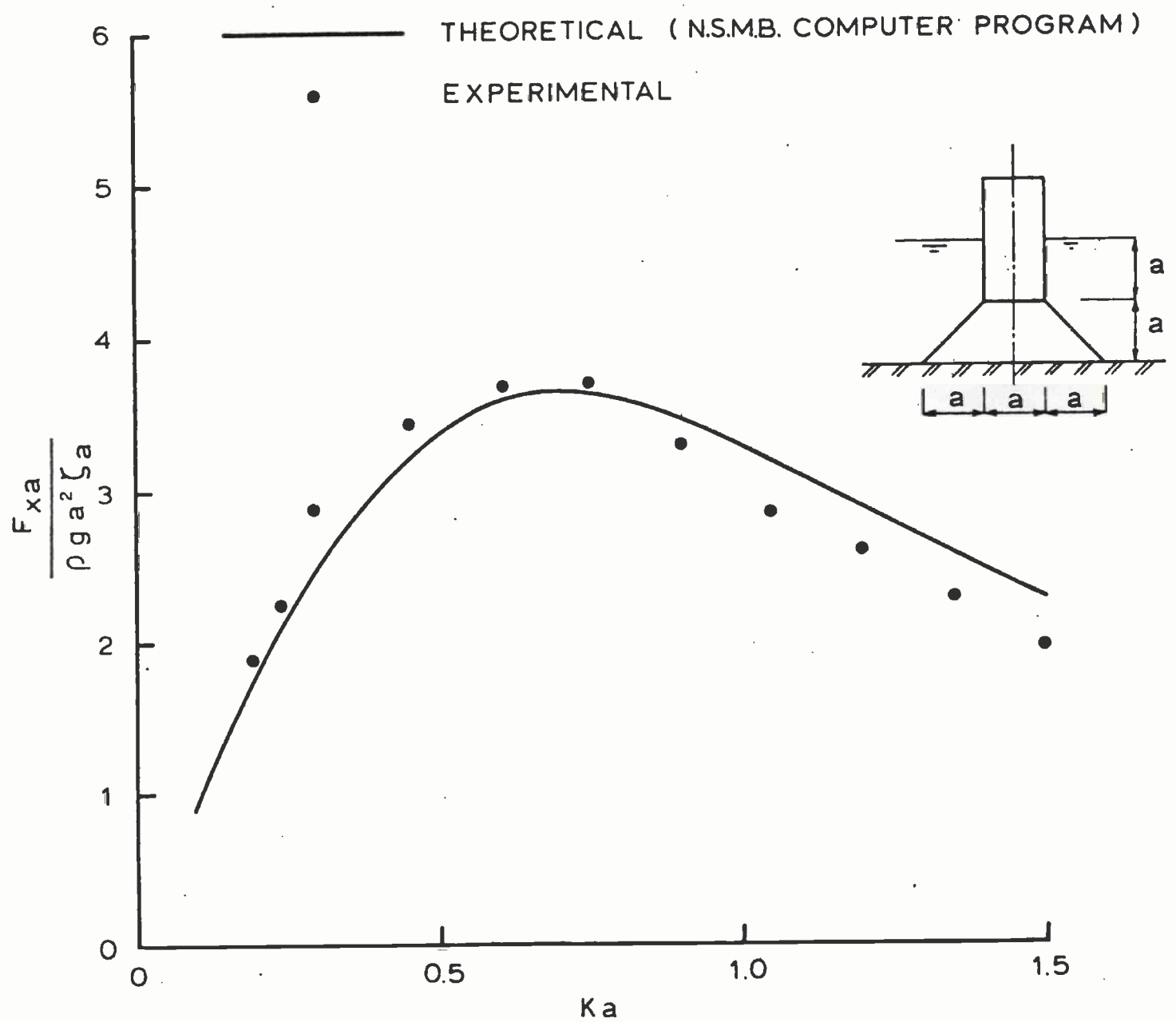


Fig. 6 The oscillating horizontal wave force on a pyramid.

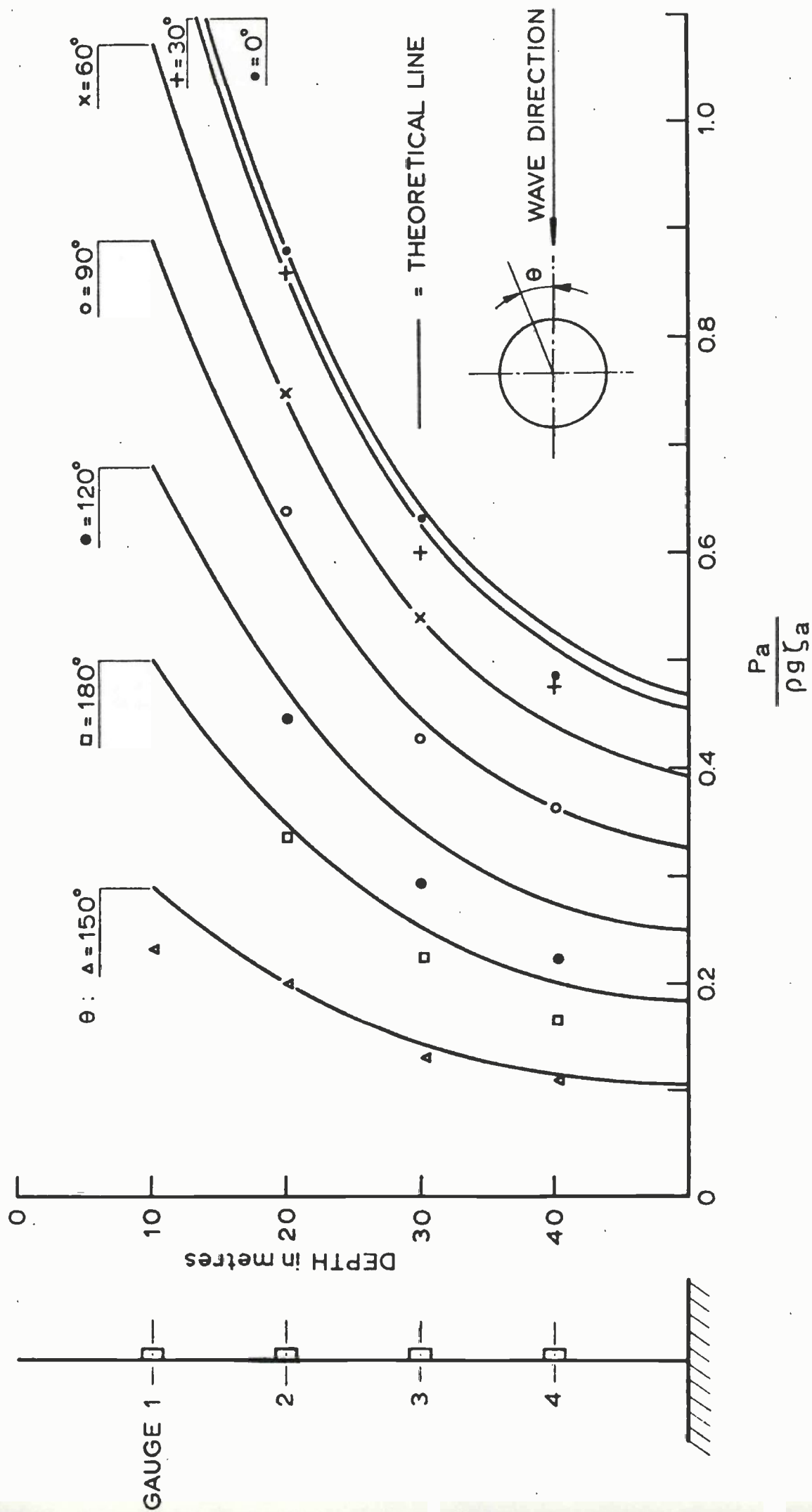


Fig. 7 Pressure on a circular cylinder in waves,  $ka = 2$

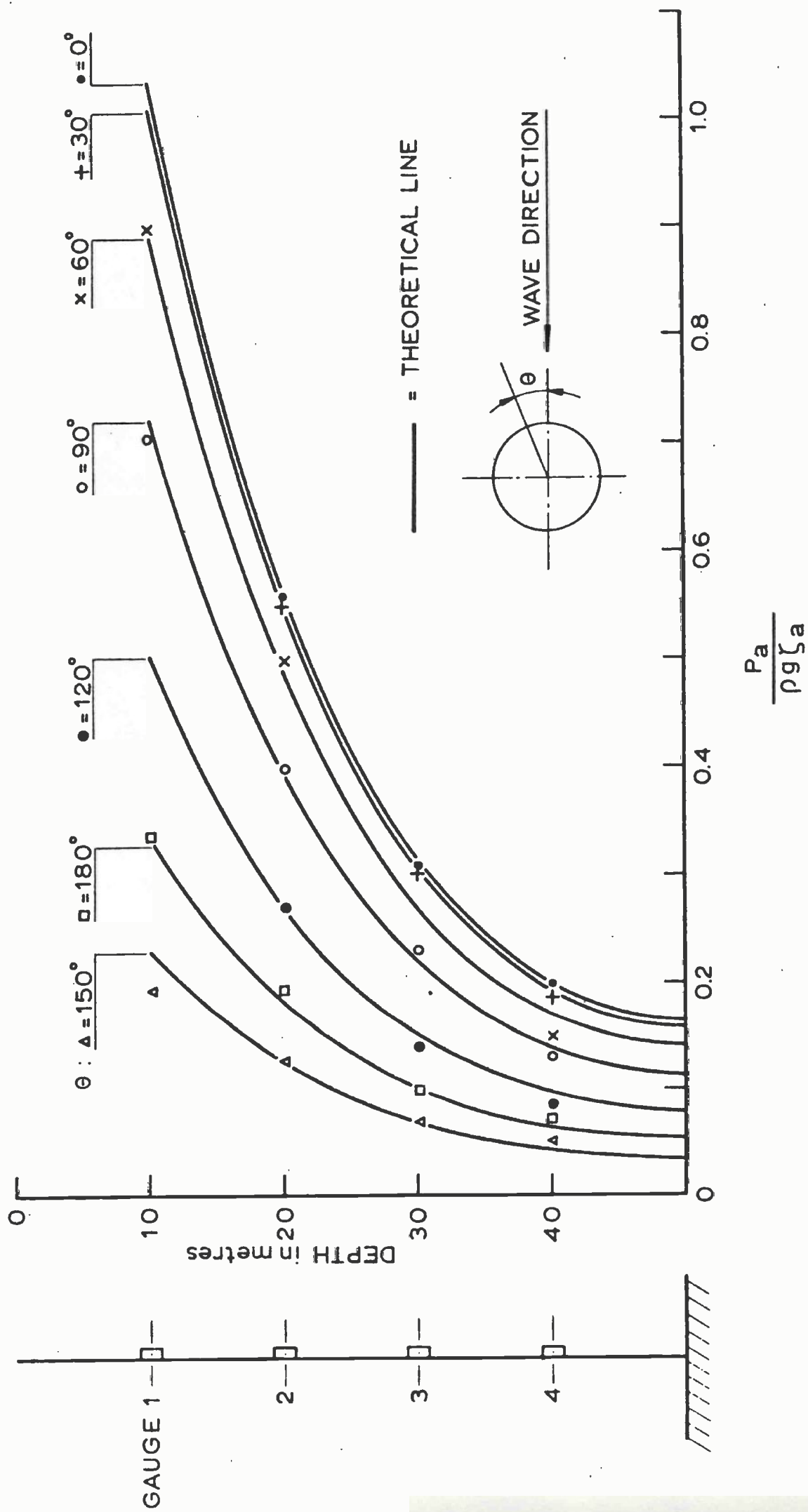


Fig. 8 Pressure on a circular cylinder in waves,  $ka = 3$

DIRECTION OF WAVE  
PROPAGATION

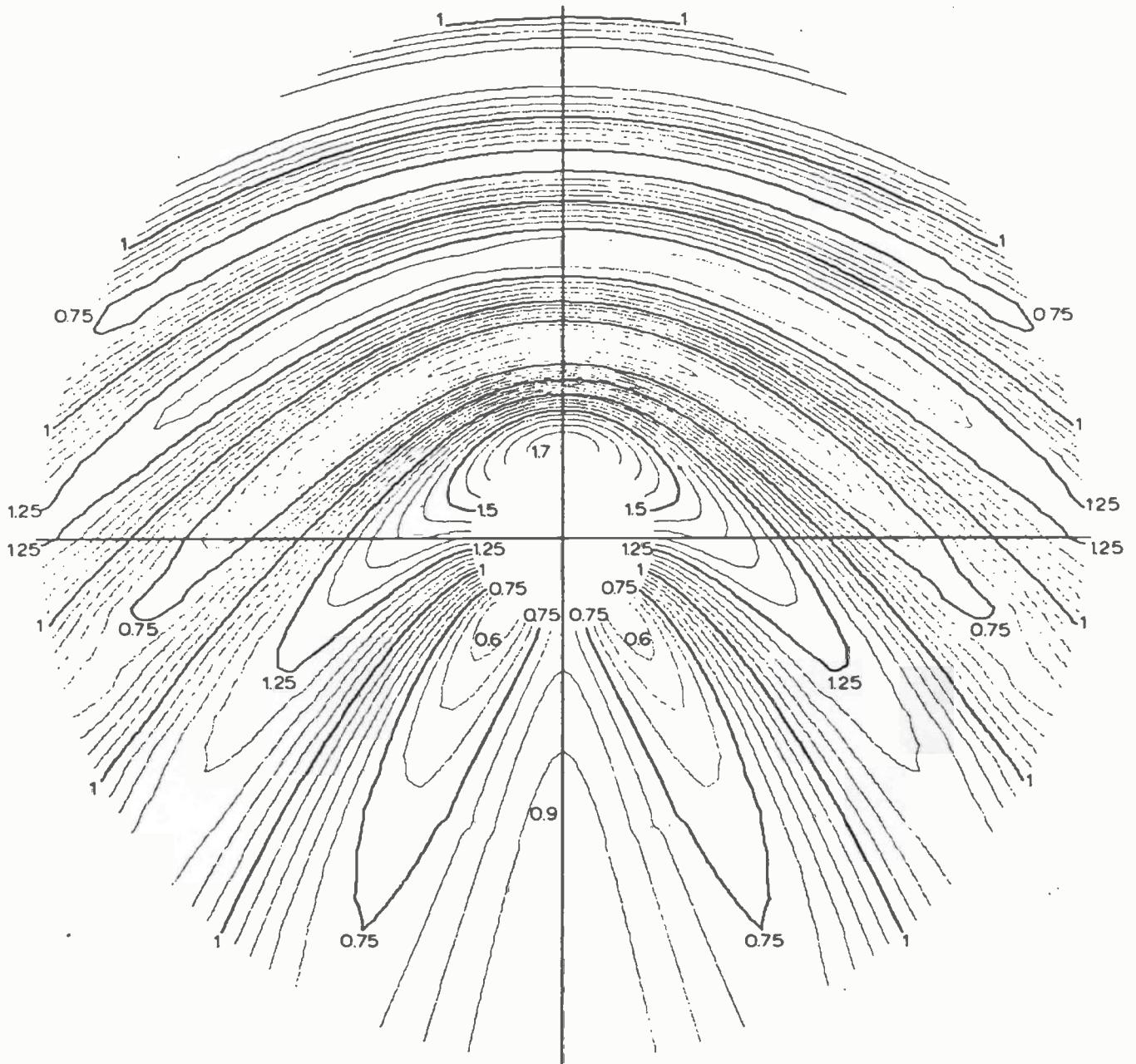


Fig. 9 Wave pattern around a circular cylinder.  
 $ka = 1.4$

$\zeta_a^*$  = ACTUAL WAVE AMPLITUDE  
 $\zeta_a$  = INCIDENT WAVE AMPLITUDE

$Ka = 4$  CYLINDER DIAMETER = 96 metres

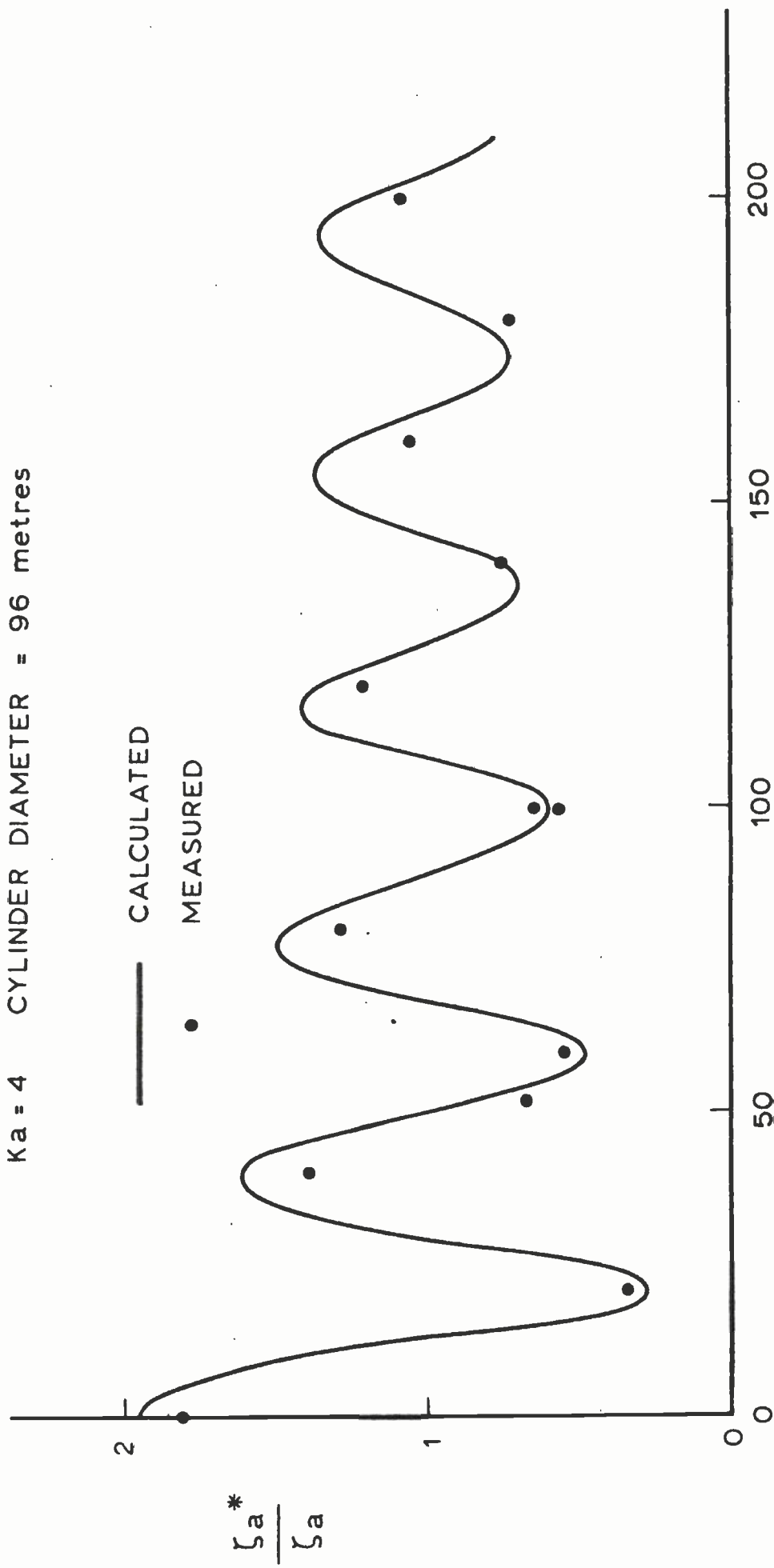


FIG. 10 The wave height in front of a circular cylinder.



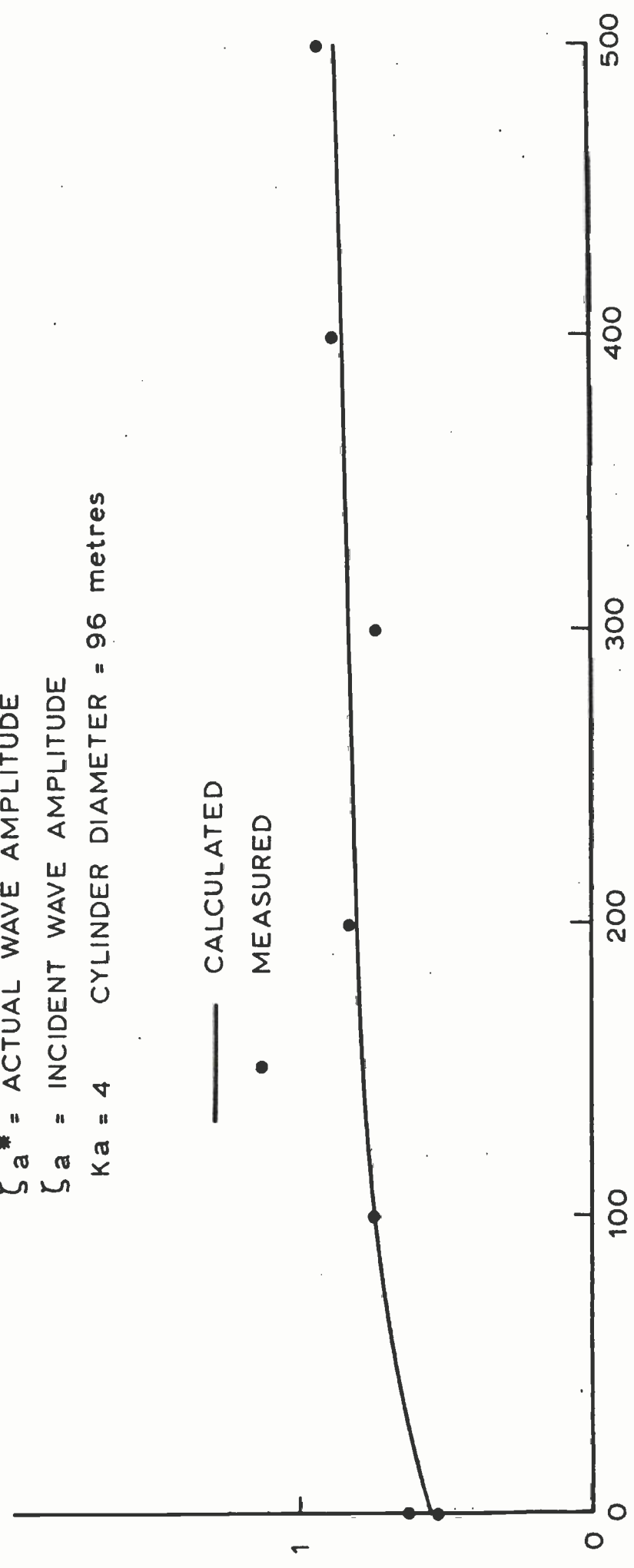
$\zeta_a^*$  = ACTUAL WAVE AMPLITUDE

$\zeta_a$  = INCIDENT WAVE AMPLITUDE

$Ka = 4$  CYLINDER DIAMETER = 96 metres

$\frac{\zeta_a^*}{\zeta_a}$

— CALCULATED  
• MEASURED



DISTANCE BEHIND THE CYLINDER IN metres

Fig. 11 The wave height behind a circular cylinder.

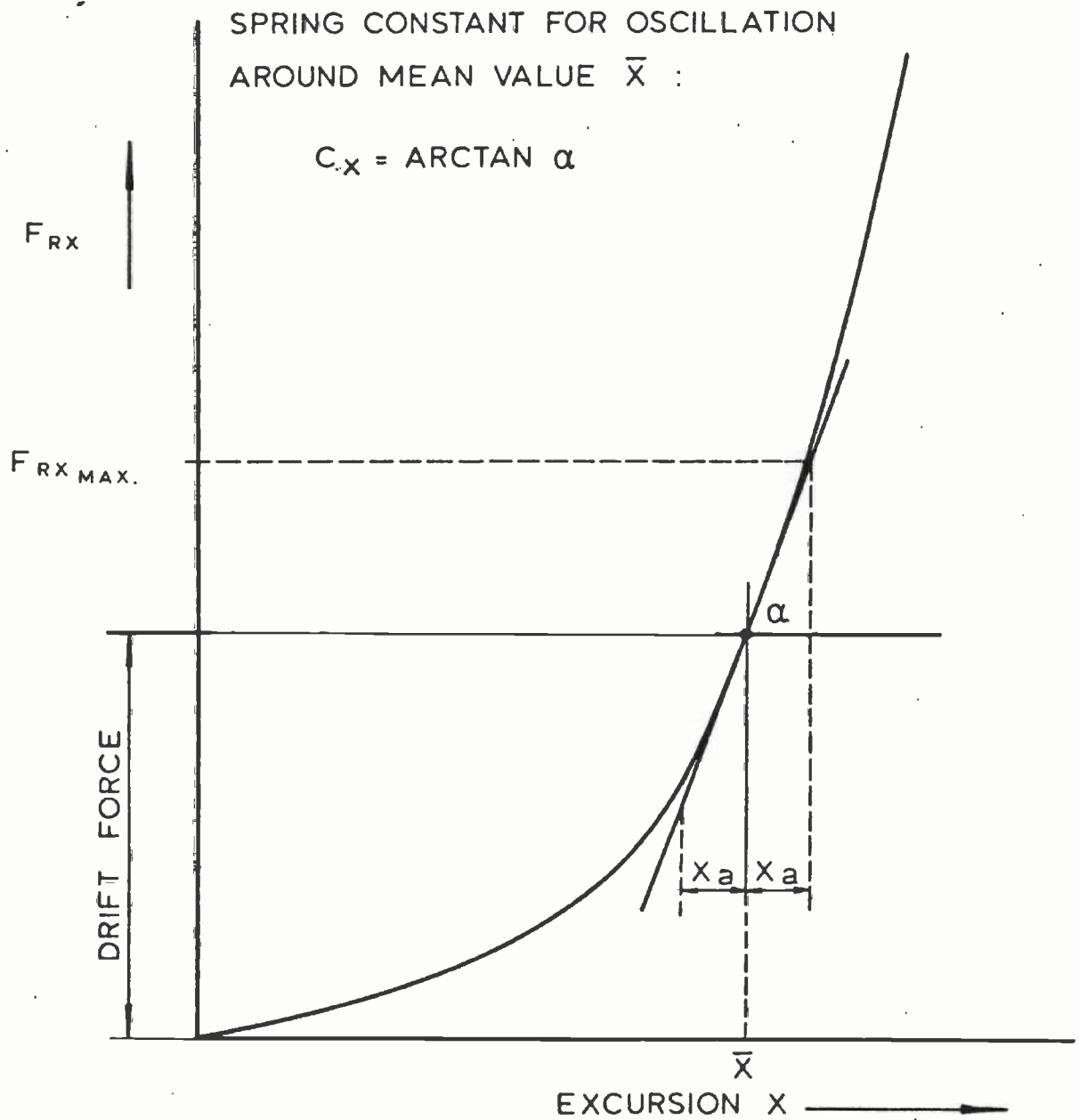


Fig. 12 Load-excitation characteristic of the anchor system.

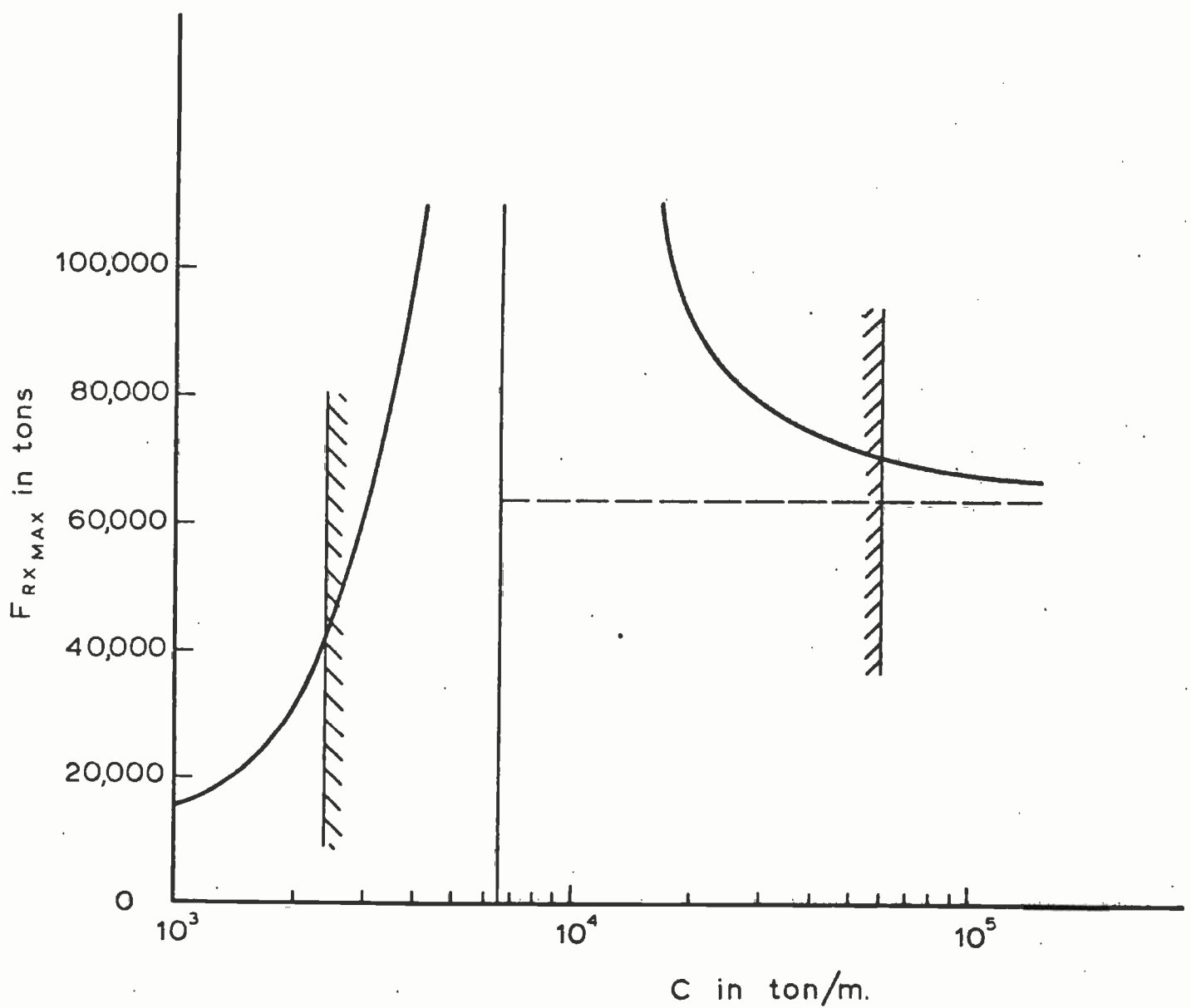


Fig. 13 Maximum horizontal reaction of the anchor system on a base of the spring constant for a design wave with wave height 20 metres, period 19 seconds.

LENGTH BETWEEN PERPENDICULARS	249.38 m.
BREADTH	37.41 m.
DRAUGHT	13.85 m.
DISPLACEMENT	106,792 m. <sup>3</sup>

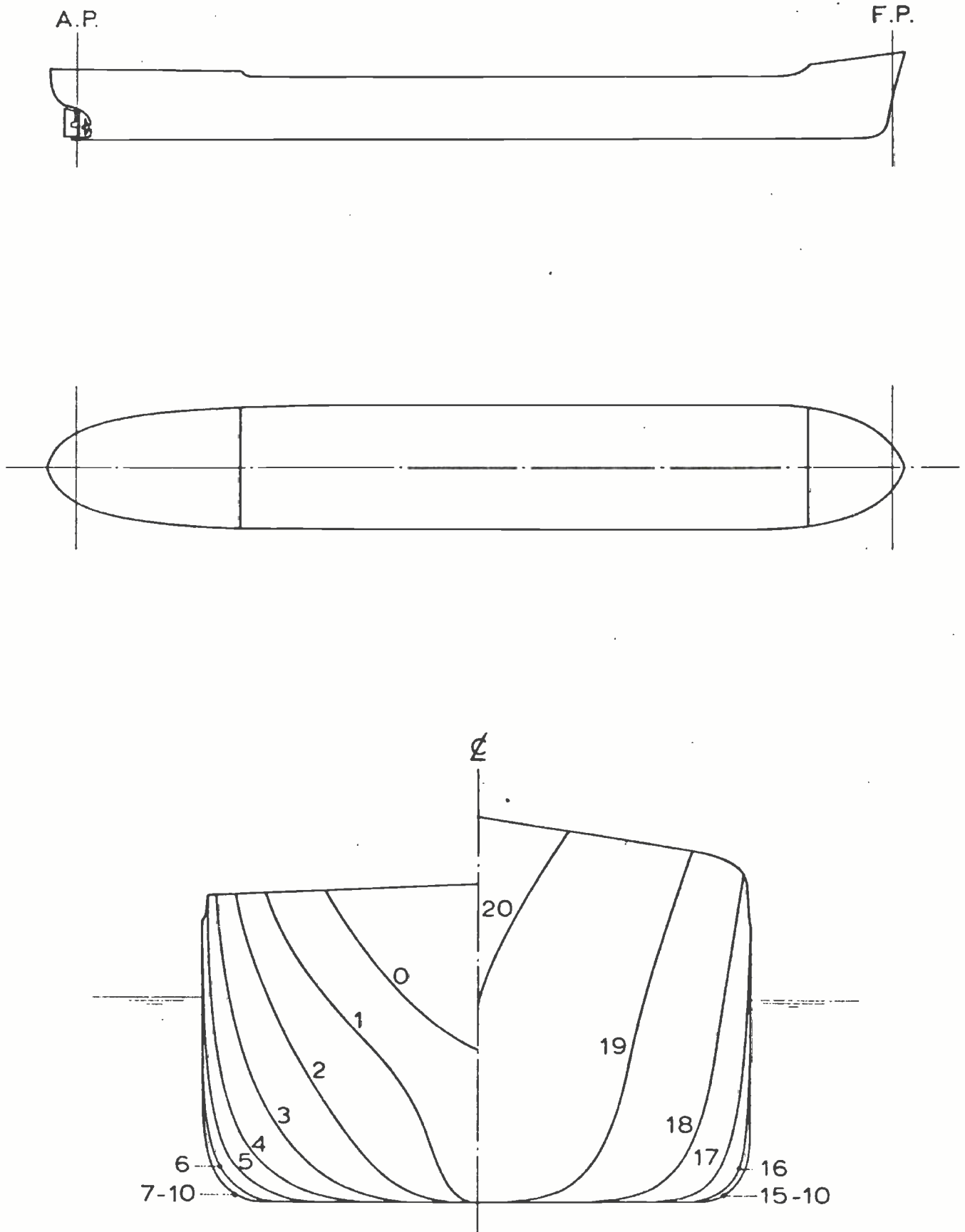


Fig. 14 Body plan of the tanker.

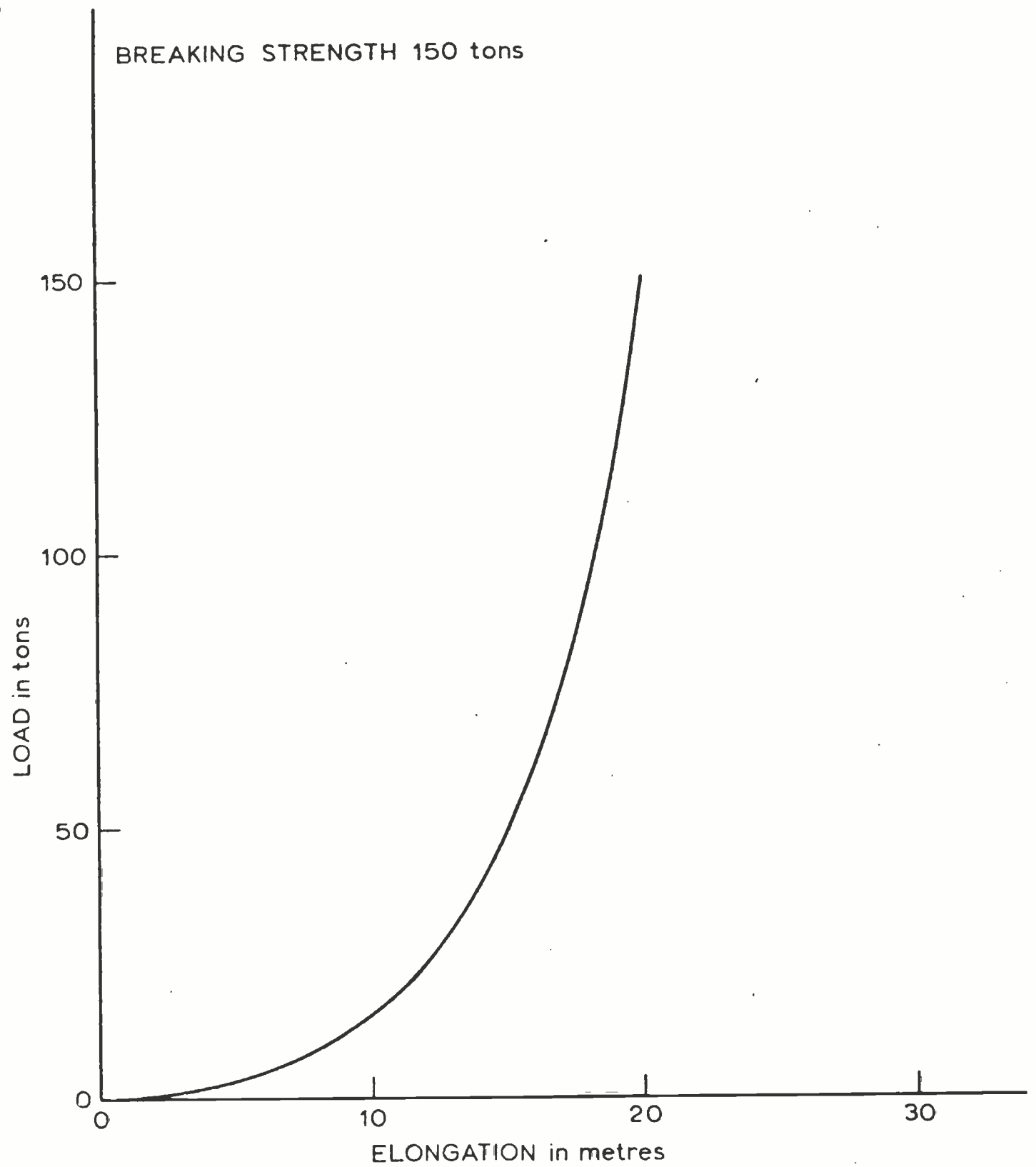
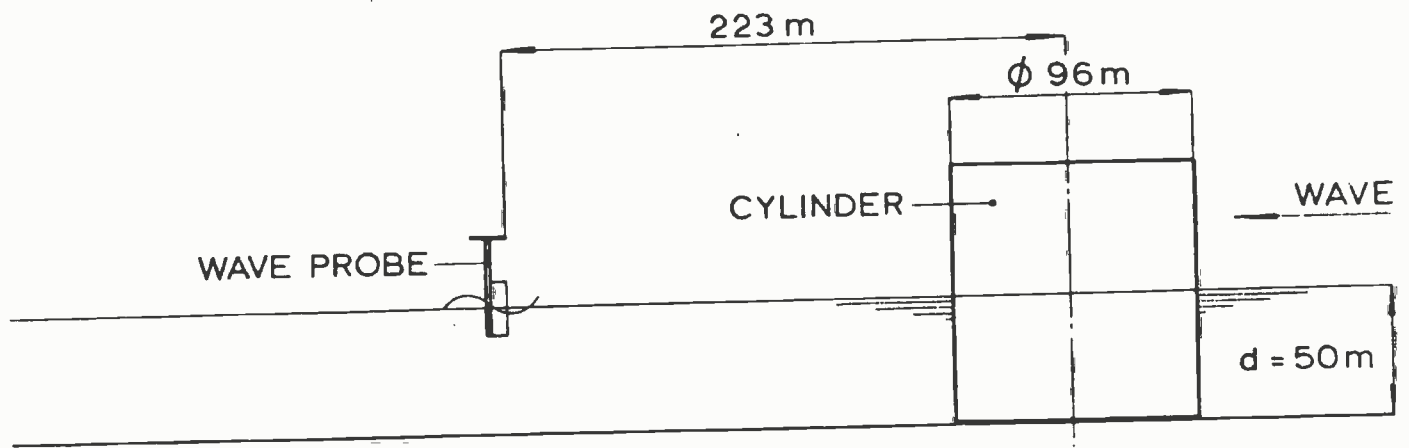
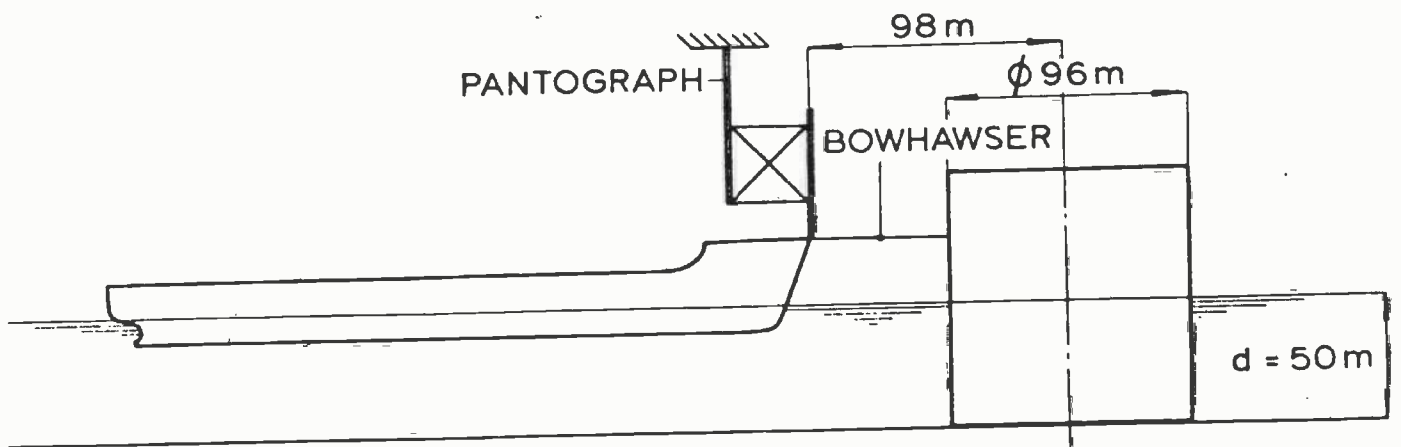


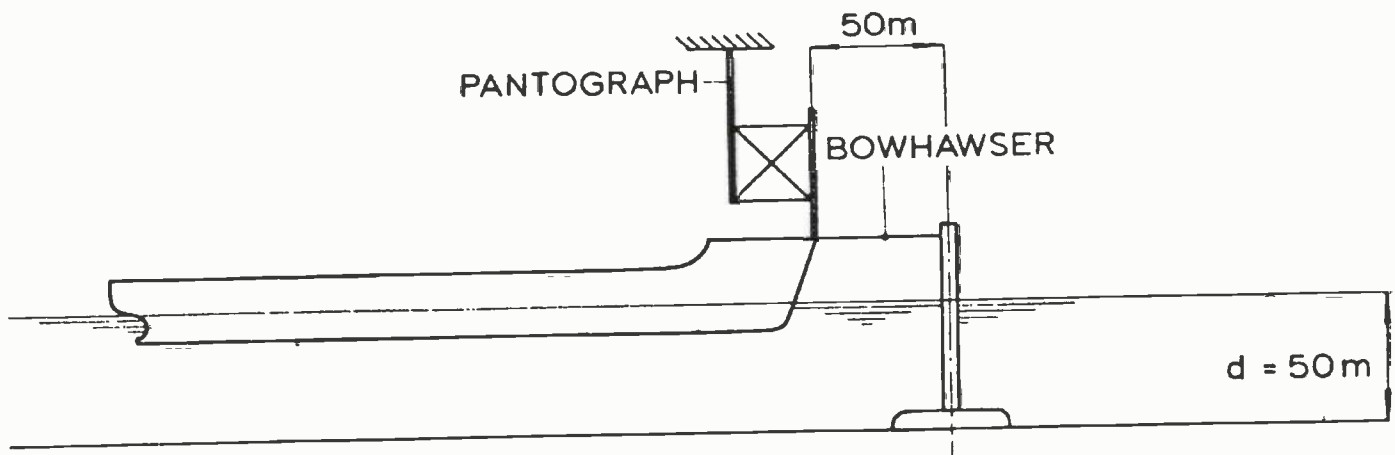
Fig. 15 The load-elongation characteristic of the bowhawser.



TEST ARRANGEMENT A



TEST ARRANGEMENT B



TEST ARRANGEMENT C

Fig. 16 The experimental set-up.

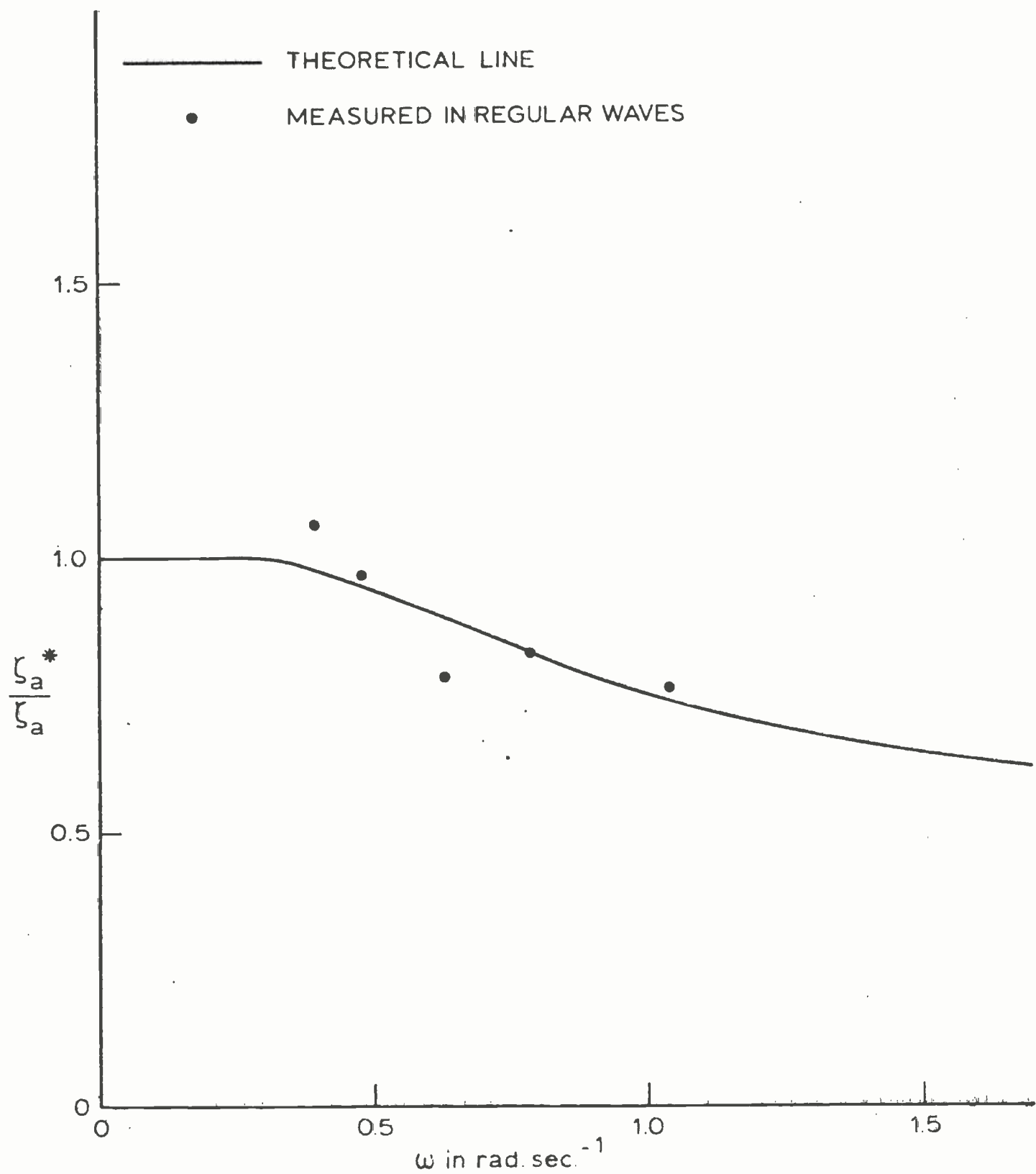


Fig. 17 Wave diffraction at the position of the tanker.

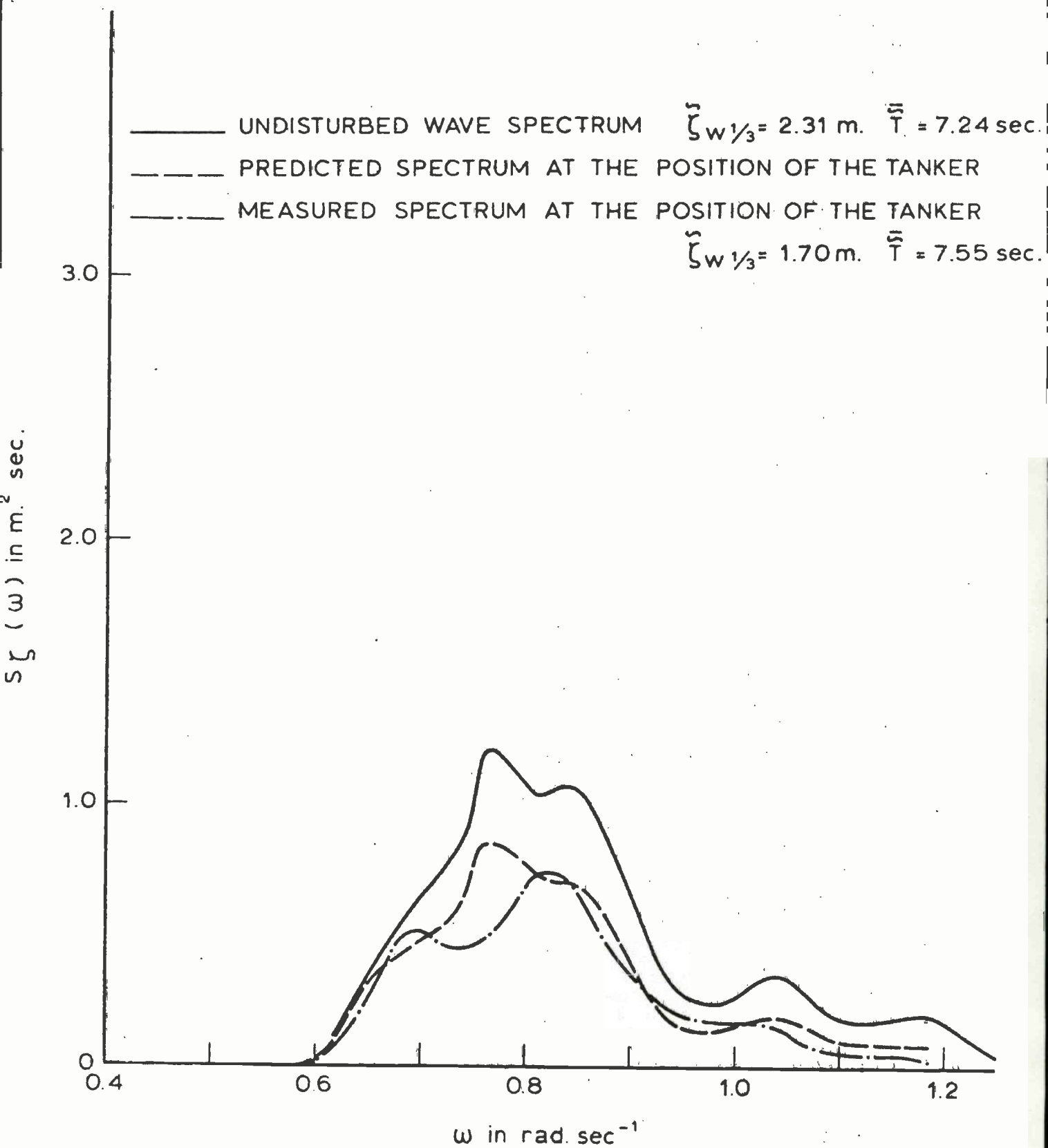


Fig. 18 Wave spectrum 1.



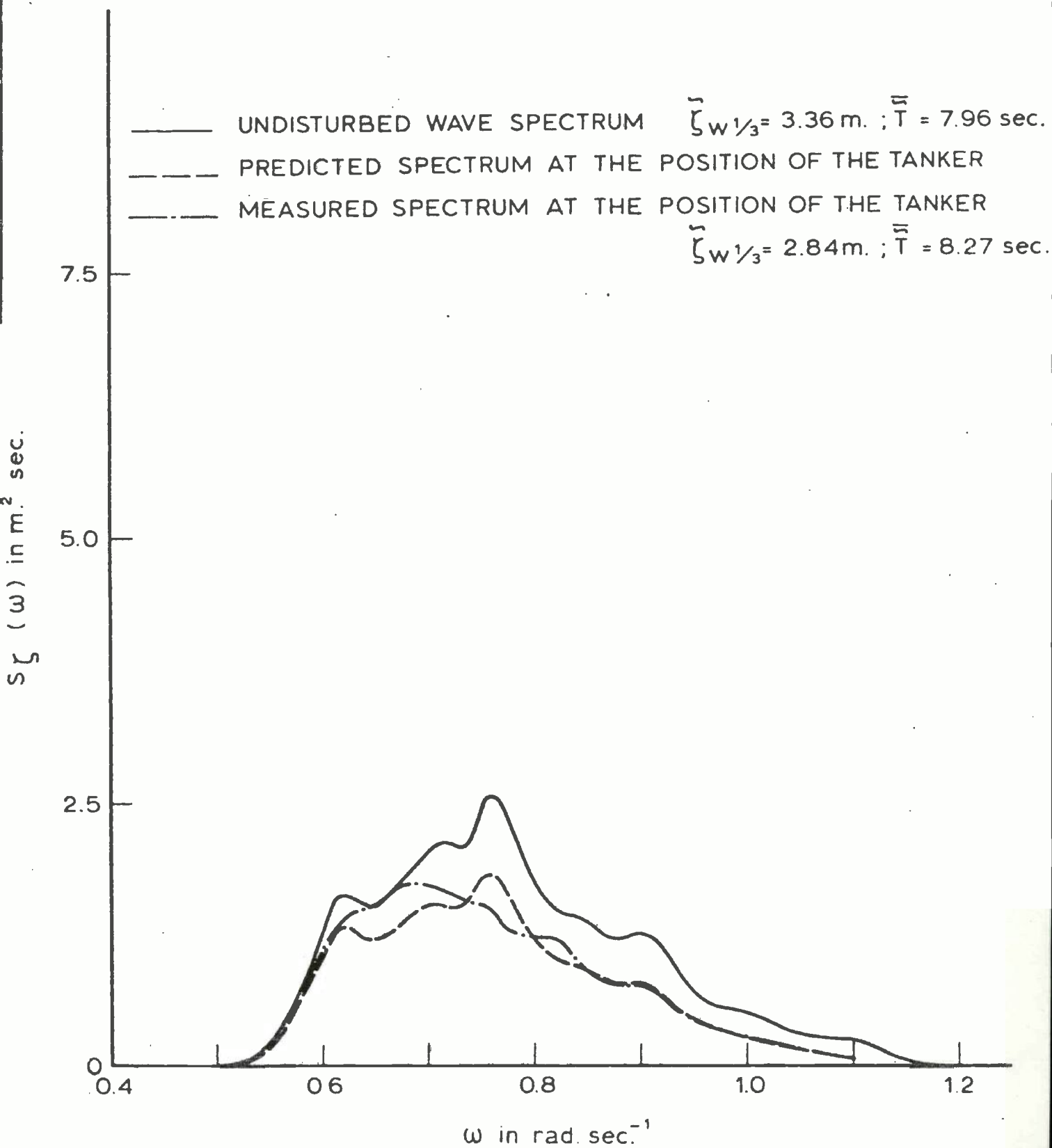


Fig. 19 Wave spectrum 2.

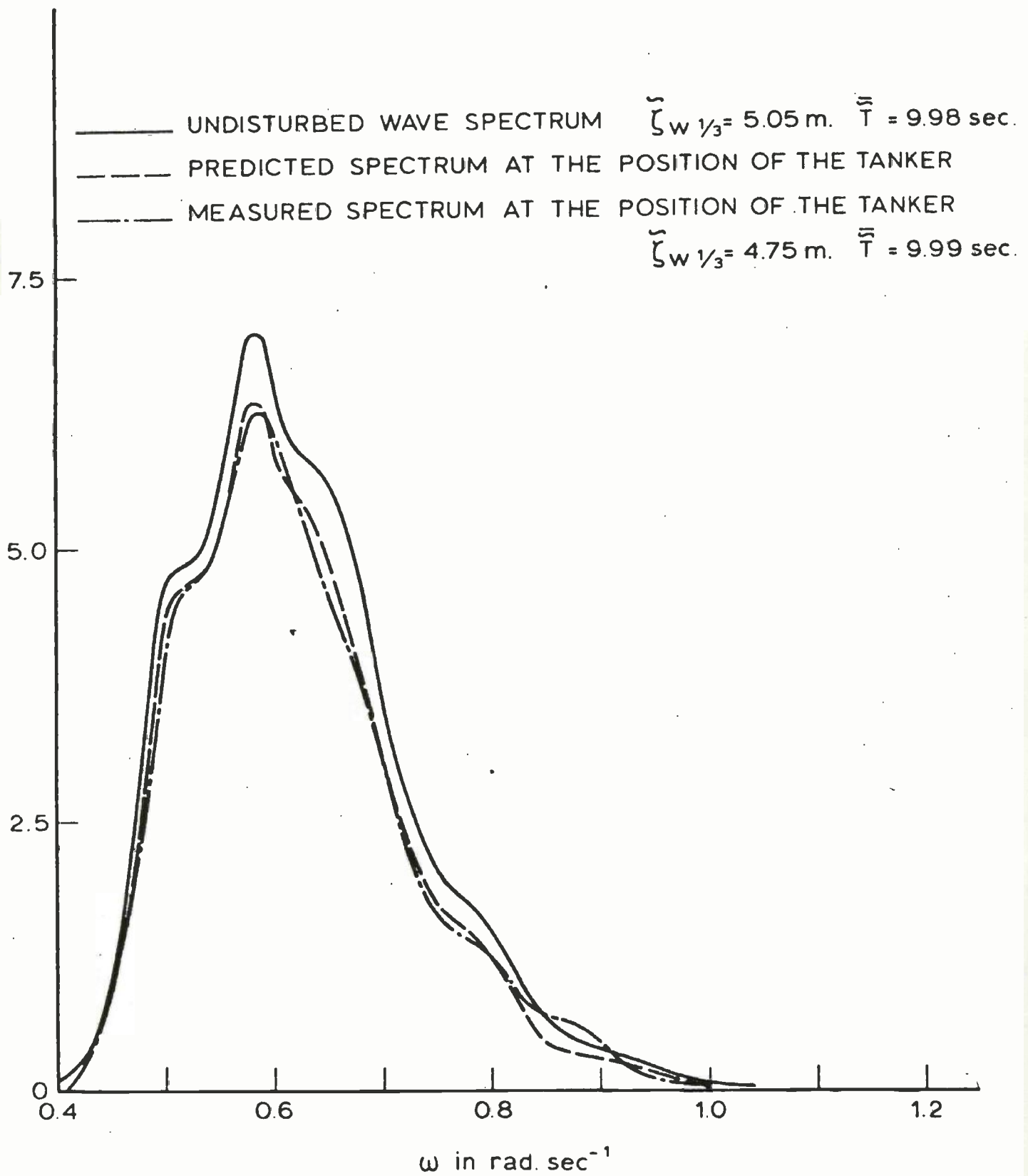


Fig. 20 Wave spectrum 3.

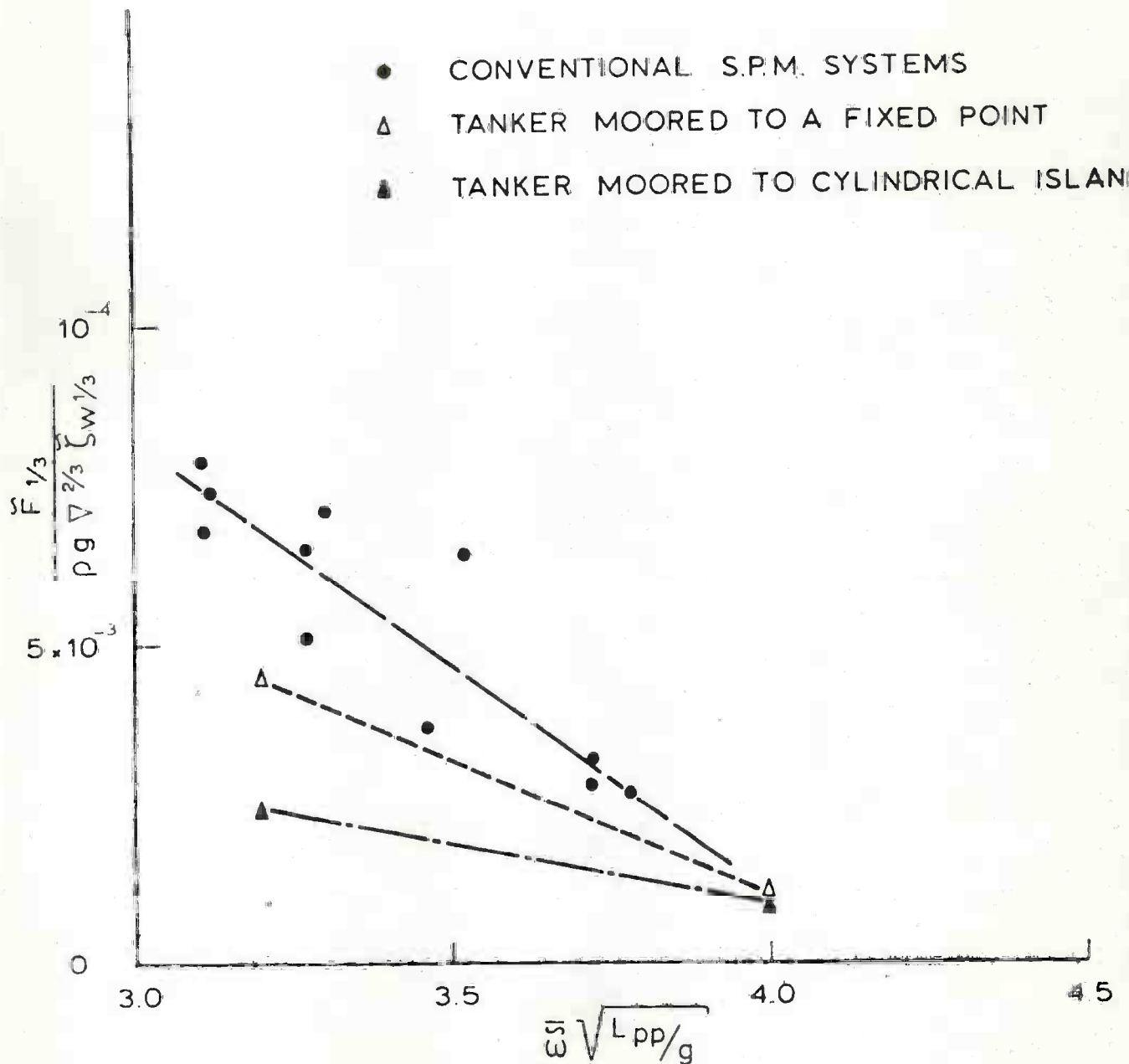


Fig. 21 The significant mooring line force for different S.P.M. systems.